noticeably change the gross appearance of the atherosclerotic lesions (66±8% in thoracic aortae and 32±7% in abdominal aortae). The immunohistochemical analysis showed that the troglitazone treatment had no significant effect on the total content of $1A4^+$ vascular smooth muscle cells (1A4-positive area/atheromatous area: 11.4±3.9% in

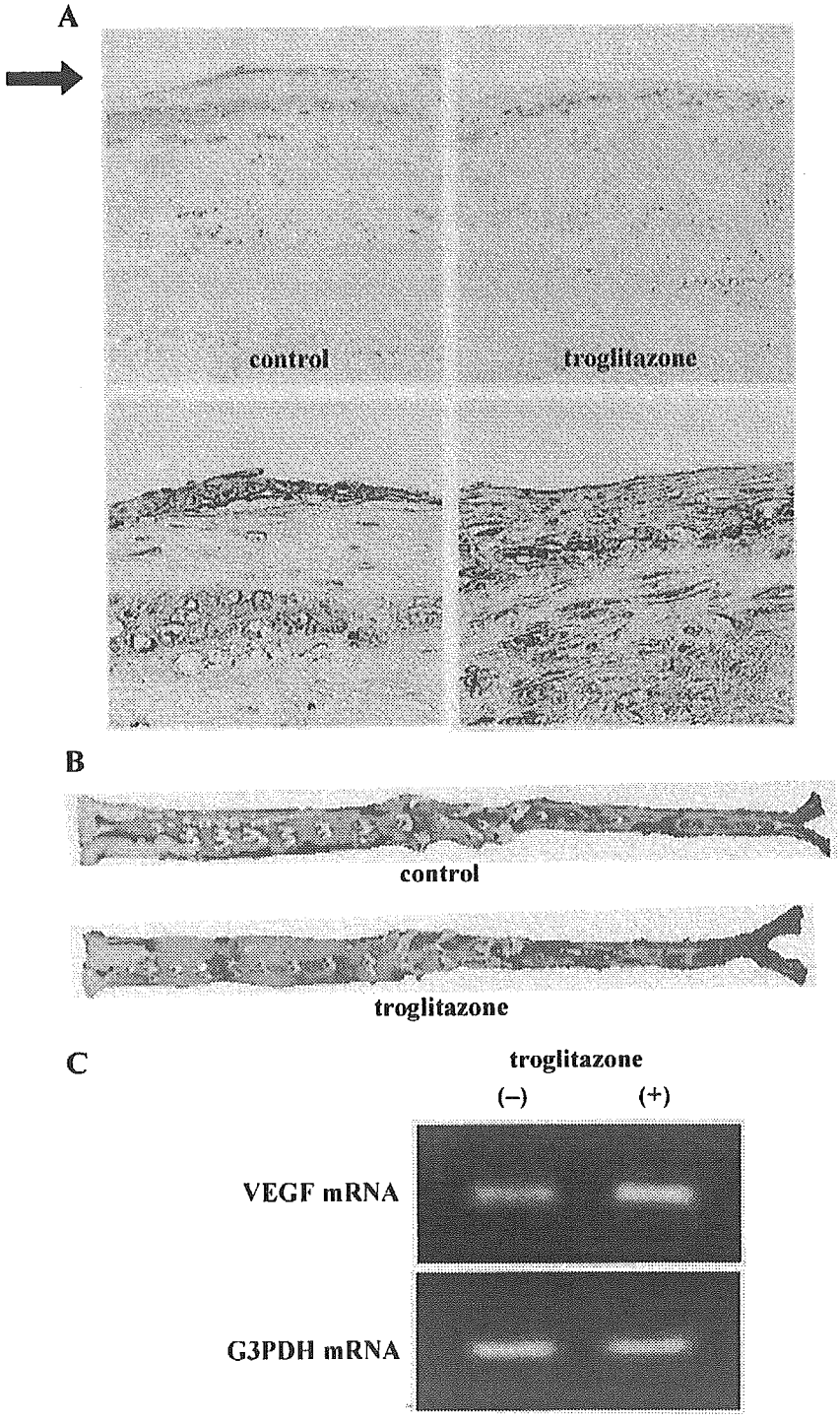

Fig. 7. Effect of troglitazone administration to balloon-injured WHHL rabbits. (A) Suppression of recruitment of monocytes/macrophages onto the surface of the aorta of WHHL rabbits 6 weeks after balloon injury. Troglitazone was administered every day for 8 weeks, from 2 weeks before injury until sampling. RAM11-positive immunostaining shows monocytes/macrophages in brown. Top: Lower magnification of the whole blood vessel. Bottom: Higher magnification of the surface of the balloon-injured aortas (the portion indicated by arrow in top). (B) Macroscopic appearance of balloon-injured aortas of WHHL rabbits after the injury. Area of re-endothelialization is not stained by Evans blue dye and appears white. Control: vehicle-treated group; troglitazone: troglitazone-treated group. (C) Analysis of VEGF gene expression. Pooled frozen aortic samples (vehicle-treated group: n=6; troglitazone-treated group: n=8) were subjected to RT-PCR for VEGF.

the abdominal and 9.3±1.1% in the thoracic aortae of the control group; 6.3±0.7% in the abdominal and 7.8±1.7% in the thoracic aortae of the troglitazone-treated group), although there was a tendency for the vascular smooth muscle cell content to decrease as a result of the troglitazone treatment, which is compatible with the results of previous studies with different experimental protocols (Shiomi et al., 1999; Law et al., 1996). Nor did the treatment significantly affect the total content of RAM11$^+$ monocytes/macrophages (RAM11-positive area/atheromatous area: 11.6±3.7% in the thoracic and 14.3±4.8% in the abdominal aortae of the control group; 14.9±3.1% in the thoracic and 12.8±2.5% in the abdominal aortae of the troglitazone-treated group).

However, the number of acutely recruited monocytes/macrophages onto the surface of the balloon injured aorta was significantly lower in the abdominal aorta of the troglitazone-treated group (39±5% of the control, $P<0.05$), although in the thoracic aorta of this group the reduction in numbers did not reach statistical significance (82±7% of the control) (Fig. 7A).

3.8. Re-endothelialization in balloon-injured aorta of WHHL rabbits accelerated by troglitazone

Evans blue staining demonstrated that the denuded area was significantly smaller in the aorta of the troglitazone-treated group than of the control group (Fig. 7B; Evans blue-stained area/non-atheromatous area: 0.4±0.2% for the troglitazone-treated and 4.8±1.2% for the control group; $P<0.05$). RT-PCR for VEGF showed that VEGF gene expression had increased in the aorta of the troglitazone-treated group (Fig. 7C).

4. Discussion

The study presented here demonstrated that PPARγ and retinoid X receptor ligands caused a concentration-dependent suppression of cell growth in PPARγ-expressing THP-1 cells. In contrast, troglitazone and 9-*cis*-retinoic acid had no effect on the proliferation of wild-type U937 which lack PPARγ expression. We further demonstrated that U937 cell lines with stable PPARγ expression restored the responsiveness to troglitazone and 9-*cis*-retinoic acid for growth suppression. These findings indicate that activation of PPARγ in monocytes/macrophages causes growth suppression of these cell lines.

We could also demonstrate that PPARγ and retinoid X receptor specific ligands strongly inhibited the MCP-1-induced migration of THP-1. This result is compatible with those reported in previous publications (Zhu et al., 1999; Kintscher et al., 2000). To investigate the potential mechanism of inhibition of MCP-1-induced migration by PPARγ activation, we also examined changes in the functional expression of CCR2 in THP-1. We found that troglitazone, 15-deoxy-Δ12,14-prostaglandin J2 and 9-*cis*-retinoic acid had a strong down-regulatory effect on CCR2 mRNA expression at the transcriptional level. We further confirmed that MCP-1 binding activity was also reduced and the number of MCP-1 receptors (CCR2) declined as a result of exposure to troglitazone and 9-*cis*-retinoic acid. Since it has been reported that in an in vitro chemotaxis assay, monocytes derived from CCR2 knockout mice failed to migrate in response to MCP-1 (Boring et al., 1997), the suppressive action of PPARγ and retinoid X receptor ligands on MCP-1-induced migration can be interpreted as representing the down-regulation of CCR2 expression.

Other studies have demonstrated that CCR2 or MCP-1 knockout mice are less susceptible to atherosclerosis and showed low monocyte recruitment in vascular lesions (Boring et al., 1998; Gu et al., 1998). The potent suppressive action of PPARγ and retinoid X receptor ligands on MCP-1-induced migration of THP-1 observed in our study suggests therefore the protective role of PPARγ in the development of atherosclerosis.

We also investigated in vivo the therapeutic effectiveness of troglitazone on acute recruitment of monocytes/macrophages onto the atheromatous lesion after balloon injury in WHHL rabbits. Since we utilized 10-month-old WHHL rabbits with fully developed atherosclerosis to examine the effect of troglitazone on the acute recruitment of monocytes onto atheromatous lesions, the effect of troglitazone on pre-existing atheromas was not as prominent as that reported by another study, which examined the effect of troglitazone on the development of atherosclerosis in younger WHHL rabbits (Shiomi et al., 1999). However, compatible with the in vitro effect of thiazolidinediones on monocytes/macrophages observed in our study, we also found in vivo evidence of suppression of acute adhesion and/or subsequent transendothelial migration in response to troglitazone treatment. Han et al. (2000) recently showed that oxLDL reduces circulating monocyte CCR2 expression through activation of PPARγ and postulated that oxLDL may promote the arrest of newly recruited monocytes in the arterial wall. However, our findings contradict their hypothesis, that is, the administration of the PPARγ agonist suppressed attachment and/or proliferation of monocytes/macrophages on atherosclerotic lesions at the site of balloon injury.

A previous study of ours found that thiazolidinediones stimulate endothelial proliferation and induce regeneration in vitro within clinically relevant doses (Fukunaga et al., 2001). The significant acceleration of re-endothelialization in the aorta after balloon injury observed in the study presented here was thus highly compatible with our previous in vitro findings. Accelerated re-endothelialization may be ascribed to the enhanced expression of pro-angiogenic factors previously demonstrated by us (Inoue et al., 2001; Itoh et al., 1999). In fact, troglitazone administration used in the current study showed increased gene expression of VEGF in the aorta of the WHHL rabbits.

In conclusion, we showed that PPARγ and retinoid X receptor specific ligands inhibited proliferation and migration of monocytes/macrophages as well as suppressed the functional expression of the MCP-1 receptor, CCR2 in THP-1. The administration of thiazolidinediones to WHHL rabbits inhibited monocyte/macrophage recruitment and induced endothelial regeneration after balloon injury. These results indicate the involvement of PPARγ in modulating monocyte proliferation, recruitment and transmigration through the endothelial cell layers under various pathological conditions and suggest the therapeutic potential of thiazolidinediones for diabetic vascular complications, which has been implied by some human studies (Minamikawa et al., 1998).

Acknowledgements

This work was supported in part by research grants from the Japanese Ministry of Education, Science and Culture, the Japanese Society for the Promotion of Science's 'Research for the Future' program (JSPS-RFTF 96100204, JSPS-RFTF 98L00801), and the Japan Smoking Research Foundation.

References

Boring, L., Gosling, J., Chensue, S.W., Kunkel, S.L., Farese Jr., R.V., Broxmeyer, H.E., Charo, I.F., 1997. Impaired monocyte migration and reduced type 1 (Th1) cytokine responses in C-C chemokine receptor 2 knockout mice. J. Clin. Invest. 100, 2552–2561.

Boring, L., Gosling, J., Cleary, M., Charo, I.F., 1998. Decreased lesion formation in CCR2−/− mice reveals a role for chemokines in the initiation of atherosclerosis. Nature 394, 894–897.

Charo, I.F., Myers, S.J., Herman, A., Franci, C., Connolly, A.J., Coughlin, S.R., 1994. Molecular cloning and functional expression of two monocyte chemoattractant protein-1 receptors reveals alternative splicing of the carboxyl-terminal tails. Proc. Natl. Acad. Sci. U. S. A. 191, 2752–2756.

Chen, Z., Ishibashi, S., Perrey, S., Osuga, J., Gotoda, T., Kitamine, T., Tamura, Y., Okazaki, H., Yahagi, N., Iizuka, Y., Shionoiri, F., Ohashi, K., Harada, K., Shimano, H., Nagai, R., Yamada, N., 2001. Troglitazone inhibits atherosclerosis in apolipoprotein E-knockout mice. Arterioscler. Thromb. Vasc. Biol. 21, 372–377.

Collins, A.R., Meehan, W.P., Kintscher, U., Jackson, S., Wakino, S., Noh, G., Palinski, W., Hsueh, W.A., Law, R.E., 2001. Troglitazone inhibits formation of early atherosclerotic lesions in diabetic and nondiabetic low density lipoprotein receptor-deficient mice. Arterioscler. Thromb. Vasc. Biol. 21, 365–371.

DeFronzo, R.A., Ferrannini, E., 1991. Insulin resistance: a multifaceted syndrome responsible for NIDDM, obesity, hypertension, dyslipidemia and atherosclerotic cardiovascular disease. Diabetes Care 14, 173–194.

Doi, K., Ikeda, T., Itoh, H., Ueyama, K., Hosoda, K., Ogawa, Y., Yamashita, J., Chun, T.-H., Inoue, M., Masatsugu, K., Sawada, N., Fukunaga, Y., Saito, T., Sone, M., Yamahara, K., Kook, H., Komeda, M., Ueda, M., Nakao, K., 2001. C-type natriuretic peptide induces redifferentiation of vascular smooth muscle cells with accelerated reendothelialization. Arterioscler. Thromb. Vasc. Biol. 21, 930–936.

Fukunaga, Y., Itoh, H., Doi, K., Tanaka, T., Yamashita, J., Chun, T.-H., Inoue, M., Masatsugu, K., Sawada, N., Saito, T., Hosoda, K., Kook, H., Ueda, M., Nakao, K., 2001. Thiazolidinediones, peroxisome proliferator-activated receptor γ agonists, regulate endothelial cell growth and secretion of vasoactive peptides. Atherosclerosis 158, 113–119.

Gu, L., Okada, Y., Clinton, S.K., Gerard, C., Sukhova, G.K., Libby, P., Rollins, B.J., 1998. Absence of monocyte chemoattractant protein-1 reduces atherosclerosis in low density lipoprotein receptor-deficient mice. Mol. Cell 2, 275–281.

Han, K.H., Chang, M.K., Boullier, A., Green, S.R., Li, A., Glass, C.K., Quenhenberger, O., 2000. Oxidized LDL reduces monocyte CCR2 expression through pathways involving peroxisome proliferator-activated receptor-γ. J. Clin. Invest. 106, 793–802.

Inoue, M., Itoh, H., Ueda, M., Naruko, T., Kojima, A., Komatsu, R., Doi, K., Ogawa, Y., Tamura, N., Takaya, K., Igaki, T., Yamashita, J., Chun, T.-H., Masatsugu, K., Becker, A.E., Nakao, K., 1998. Vascular endothelial growth factor (VEGF) expression in human coronary atherosclerotic lesions: possible pathophysiological significance of VEGF in progression of atherosclerosis. Circulation 98, 2108–2116.

Inoue, M., Itoh, H., Tanaka, T., Chun, T.-H., Doi, K., Fukunaga, Y., Sawada, N., Yamashita, J., Masatsugu, K., Saito, T., Sakaguchi, S., Sone, M., Yamahara, K., Yurugi, T., Nakao, K., 2001. Oxidized low density lipoprotein regulates VEGF expression in human macrophages and endothelial cells through activation of PPARγ. Arterioscler. Thromb. Vasc. Biol. 21, 560–566.

Itoh, H., Doi, K., Tanaka, T., Fukunaga, Y., Hosoda, K., Inoue, G., Nishimura, H., Yoshimasa, Y., Yamori, Y., Nakao, K., 1999. Hypertension and insulin resistance—the role of peroxisome proliferator-activated receptor-γ. Clin. Exp. Pharmacol. Physiol. 26, 558–560.

Kintscher, U., Goetze, S., Wakino, S., Kim, S., Nagpal, S., Chandraratna, R.A.S., Graf, K., Fleck, E., Hsueh, W.A., Law, R.E., 2000. Peroxisome proliferator-activated receptor and retinoid X receptor ligands inhibit monocyte chemotactic protein-1-directed migration of monocytes. Eur. J. Pharmacol. 401, 259–270.

Law, R.E., Meehan, W.P., Xi, X.-P., Graf, K., Wuthrich, D.A., Coats, W., Faxon, D., Hsueh, W.A., 1996. Troglitazone inhibits vascular smooth muscle cell growth and intimal hyperplasia. J. Clin. Invest. 98, 1897–1905.

Lehmann, J.M., Moore, L.B., Smith-Oliver, T.A., Wilkinson, W.O., Willson, T.M., Kliewer, S.A., 1995. An antidiabetic thiazolidinedione is a high affinity ligand for peroxisome proliferator-activated receptor gamma (PPAR gamma). J. Biol. Chem. 270, 12953–12956.

Minamikawa, J., Tanaka, S., Yamauchi, M., Inoue, D., Koshiyama, H., 1998. Potent inhibitory effect of troglitazone on carotid arterial wall thickness in type 2 diabetes. J. Clin. Endocrinol. Metab. 83, 1818–1820.

Nagy, L., Tontonoz, P., Alvarez, J.G.A., Chen, H., Evans, R.M., 1998. Oxidized LDL regulates macrophage gene expression through ligand activation of PPARgamma. Cell 93, 229–240.

Nelken, N.A., Coughlin, S.R., Gordon, D., Wilcox, J.N., 1991. Monocyte chemoattractant protein-1 in human atheromatous plaques. J. Clin. Invest. 88, 1121–1127.

Nolan, J.J., Ludvik, B., Beerdsen, P., Joyce, M., Olefsky, J., 1994. Improvement in glucose tolerance and insulin resistance in obese subjects treated with troglitazone. N. Engl. J. Med. 331, 1188–1193.

Ricote, M., Li, A.C., Willson, T.M., Kelly, C.J., Glass, C.K., 1998. The peroxisome proliferator-activated receptor-gamma is a negative regulator of macrophage activation. Nature 391, 79–82.

Sawada, N., Itoh, H., Ueyama, K., Yamashita, J., Doi, K., Chun, T.-H., Inoue, M., Masatsugu, K., Saito, T., Fukunaga, Y., Sakaguchi, S., Arai, H., Ohno, N., Komeda, M., Nakao, K., 2000. Inhibition of Rho-associated kinase results in suppression of neointimal formation of balloon-injured arteries. Circulation 101, 2030–2033.

Shiomi, M., Ito, T., Tsukada, T., Tsujita, Y., Horikoshi, H., 1999. Combination treatment with troglitazone, an insulin action enhancer, and pravastatin, an inhibitor of HMG-CoA reductase, shows a synergistic effect on atherosclerosis of WHHL rabbits. Atherosclerosis 142, 345–353.

Skorjanc, D., Jaschinski, F., Heine, G., Pette, D., 1998. Sequential increases in capillarization and mitochondrial enzymes in low-frequency-stimulated rabbit muscle. Am. J. Physiol. 274, C810–C818.

Tanaka, T., Itoh, H., Doi, K., Fukunaga, Y., Hosoda, K., Shintani, M., Yamashita, J., Chun, T.-H., Inoue, M., Masatsugu, K., Sawada, N., Saito, T., Inoue, G., Nishimura, H., Yoshimasa, Y., Nakao, K., 1999. Down regulation of peroxisome proliferator-activated receptor gamma expression by inflammatory cytokines and its reversal by thiazolidinediones. Diabetologia 42, 702–710.

Tontonoz, P., Hu, E., Spiegelman, B.M., 1994. Stimulation of adipogenesis in fibroblasts by PPAR gamma 2, a lipid-activated transcription factor. Cell 79, 1147–1156.

Tontonoz, P., Nagy, L., Alvarez, J.G.A., Thomazy, V.A., Evans, R.M., 1998. PPARgamma promotes monocyte/macrophage differentiation and uptake of oxidized LDL. Cell 93, 241–252.

Zhu, L., Bisgaier, C.L., Aviram, M., Newton, R.S., 1999. 9-*Cis* retinoic acid induces monocytes chemoattractant protein-1 secretion in human monocytic THP-1 cells. Arterioscler. Thromb. Vasc. Biol. 19, 2105–2111.

Available online at www.sciencedirect.com

SCIENCE DIRECT

Regulatory Peptides 127 (2005) 159–167

REGULATORY PEPTIDES

www.elsevier.com/locate/regpep

Angiotensin II suppresses growth arrest specific homeobox (Gax) expression via redox-sensitive mitogen-activated protein kinase (MAPK)

Takatoshi Saito[a], Hiroshi Itoh[a,*], Jun Yamashita[a], Kentaro Doi[a], Tae-Hwa Chun[a], Tokuji Tanaka[a], Mayumi Inoue[a], Ken Masatsugu[a], Yasutomo Fukunaga[a], Naoki Sawada[a], Satsuki Sakaguchi[a], Hiroshi Arai[a], Katsuyoshi Tojo[b], Naoko Tajima[b], Tatsuo Hosoya[c], Kazuwa Nakao[a]

[a]*Department of Medicine and Clinical Science, Kyoto University Graduate School of Medicine, 54 Shogoin Kawahara-cho, Sakyo-ku, Kyoto 606-8507, Japan*
[b]*Department of Internal Medicine, Division of Diabetes and Endocrinology, the Jikei University School of Medicine, Tokyo, Japan*
[c]*Department of Internal Medicine, Division of Nephrology and Hypertension, the Jikei University School of Medicine, Tokyo, Japan*

Received 2 May 2004; received in revised form 29 October 2004; accepted 18 November 2004
Available online 18 December 2004

Abstract

Oxidative stress is known to be involved in growth control of vascular smooth muscle cells (VSMCs). We and others have demonstrated that angiotensin II (Ang II) has an important role in vascular remodeling. Several reports suggested that VSMC growth induced by Ang II was elicited by oxidative stress. Gax, growth arrest-specific homeobox is a homeobox gene expressed in the cardiovascular system. Over expression of Gax is demonstrated to inhibit VSMC growth. We previously reported that Ang II down-regulated Gax expression. To address the regulatory mechanism of Gax, we investigated the significance of oxidative stress in Ang II-induced suppression of Gax expression. We further examined the involvement of mitogen-activated protein kinases (MAPKs), which is crucial for cell growth and has shown to be activated by oxidative stress, on the regulation of Gax expression by Ang II. Ang II markedly augmented intracellular H_2O_2 production which was decreased by pretreatment with *N*-acetylcystein (NAC), an anti-oxidant. Ang II and H_2O_2 decreased Gax expression dose-dependently and these effects were blocked by administration of both NAC and pyrrolidine dithiocarbamate (PDTC), another anti-oxidant. Ang II and H_2O_2 induced marked activation of extracellular signal-responsive kinase1/2 (ERK1/2), which was blocked by NAC. Ang II and H_2O_2 also activated p38MAPK, and they were blocked by pre-treatment with NAC. However, the level of activated p38MAPK was quite low in comparison with ERK1/2. Ang II- or H_2O_2-induced Gax down-regulation was significantly inhibited by PD98059, an ERK1/2 inhibitor but not SB203580, a p38MAPK inhibitor. The present results demonstrated the significance of regulation of Gax expression by redox-sensitive ERK1/2 activation.

Keywords: Angiotensin II; Gax; Mitogen-activated protein kinase; Vascular smooth muscle cell; Oxidative stress

1. Introduction

The physiological production of reactive oxygen species (ROS) such as superoxide (O2–) and hydrogen peroxide (H_2O_2) is necessary for maintenance of normal cell function and cell homeostasis, however, surplus generation of ROS called as oxidative stress has been implicated in pathophysiological mechanism [1,2]. In vasculature, growth of vascular smooth muscle cells (VSMCs) is shown to be elicited by oxidative stress [3,4]. In contrast, treatments with antioxidants such as *N*-acetylcystein (NAC) have been reported to inhibit cell growth in cultured VSMC [5]. In vivo, advanced glycation end-products and oxidized LDL which have been shown to induce atherosclerosis via VSMC growth and migration also promote oxidative stress through intracellular ROS generation [6,7]. Moreover, some types of hypertension and development of restenosis after angioplasty are shown to be incited by oxidative stress through VSMCs growth [8]. Thus, oxidative stress seems to play a consequent role in vascular diseases.

* Corresponding author. Tel.: +81 75 751 3170; fax: +81 75 771 9452.
E-mail address: hiito@kuhp.kyoto-u.ac.jp (H. Itoh).

0167-0115/$ - see front matter © 2004 Elsevier B.V. All rights reserved.
doi:10.1016/j.regpep.2004.11.006

We and others have demonstrated that angiotensin II (Ang II) has an important role in vascular remodeling [9,10]. Recently several reports have suggested that growth stimulation of VSMC and hypertension induced by Ang II was elicited with ROS generation. Laursen et al. demonstrated that Ang II-induced hypertension was produced by an increase in endogenous free radical generation and that chronic infusion of liposome-encapsulated superoxide dismutase (SOD), a specific reductase to O2–, markedly decreased blood pressure increase by Ang II [11]. Another report has also demonstrated that Ang II-induced increase in [3H] leucine incorporation in VSMC is remarkably inhibited by overexpression of catalase, a specific reductase that converts H_2O_2 to water and oxygen, suggesting that H_2O_2 generated with Ang II stimulation was a crucial signaling in vascular hypertrophy [12]. These observation all together indicate that redox-sensitive signaling pathway is an important component in Ang II-modulated vascular remodeling, however, the mechanism underlying these effects remains still unclear.

Homeobox genes implicated in gene transcription have a crucial role in cell proliferation and migration [13]. Growth arrest-specific homeobox (Gax) widely distributed in cardiovascular system [14]. It is reported that Gax expression is suppressed with growth stimulation induced by serum or platelet-derived growth factor (PDGF) in quiescent VSMCs [14]. Microinjection of a recombinant Gax protein or overexpression of Gax by infection with an adenovirus Gax construct induces inhibition of G0/G1 cell cycle transition in a p21cip1-dependent manner in vitro and reduced vessel stenosis in a rabbit model of balloon angioplasty [15,16]. We and others revealed that vasoactive substances especially occurring within the blood vessels not only regulate vascular tone but also modulate vascular growth [17]. Vasoconstrictive peptides such as Ang II and endothelin promote vascular growth and, conversely, vasodilating substances such as natriuretic peptides (NPs) and nitric oxide inhibit vascular growth [3,18,19]. We recently demonstrated that Ang II and NPs oppositely regulate Gax expression in VSMCs [20]. However, the mechanism of the Gax regulation pathway has not been established. To address the regulation mechanism of Gax expression, we investigated the significance of ROS in Ang II-induced suppression of Gax expression. In addition, we further examined the involvement of mitogen-activated protein kinases (MAPKs), which are crucial for cell growth and have shown to be activated by ROS, in regulation of Gax expression by Ang II.

2. Material and method

2.1. Reagents

Human Ang II was purchased from Peptide Institute (Osaka, Japan). Dimethyl sulfoxide (DMSO) and NAC were obtained from *Nacalai tesque* (Kyoto, Japan). [α32-P] dCTP (3000 Ci/mmol) was obtained from Amersham International (Aylesbury, UK). PD98059, an inhibitor of extracellular signal-responsive kinase 1 and 2 (ERK1/2) kinase inhibitor, and SB203580, an inhibitor of p38MAPK, and pyrrolidine dithiocarbamate (PDTC) were obtained from Sigma (St. Louis, MO).

2.2. Cell culture

Aortic VSMCs harvested from male Wistar rats were purchased from TOYOBO and were grown in Dulbecco's modified Eagle's medium (DMEM, Nikken Bio Medical Laboratories, Tokyo, Japan) supplemented with 10% fetal calf serum (FCS, Cell culture Laboratories, Cleveland, OH, U.S.A.) with 100 U/mL penicillin and 100 μg/mL streptomycin. Cells were maintained at 37 °C in a humidified atmosphere of 95% air–5% CO_2. VSMCs from 4th to 8th passage were used in the present study.

2.3. Intracellular H_2O_2 measurement

VSMCs were plated into 10-cm-diameter dishes and grown up to about 60–80% confluent in culture medium containing 10% FCS, and made quiescent by additional 24 h in FCS free DMEM. Then, the medium was replaced with fresh DMEM and incubated for 30 min with or without NAC and for 10 min with 10 μM H_2O_2-sensitive fluorophore 2′, 7′-dichlorofluorescin diacetate (DCF-DA, Sigma) before 100 nM Ang II or 200 μM H_2O_2 treatment. Cells were stimulated with H_2O_2 or Ang II for 5 min and washed 2 times with ice-cold PBS and placed on ice. Cells were harvested with 1 mL Trypsin/EDTA and centrifuged at 2000×*g* in a microcentifuge [4] for 5 min. Cells were washed twice with ice-cold PBS and resuspended with 0.4 mL ice-cold PBS. The levels of intracellular H_2O_2 were measured by FACS Caliber (Becton Dickinson) as described elsewhere [21].

2.4. RNA preparation and Northern blot analysis

VSMCs were plated and quiescent as described above for estimation of Gax mRNA expression. Cells were pre-treated with 1 mM NAC, 50–500 μM PDTC, 30 μM PD98059, and 10 μM SB203580 or vehicle for 30 min in case of need and stimulated with various concentration of AngII and H_2O_2. Cells were incubated for 6 h and harvested for RNA isolation. Total cellular RNA extraction and estimation of Gax mRNA expression were performed as previously reported [20].

2.5. Detection of ERK1/2 phosphorylation by immunobloting

VSMCs were plated and quiescent as described above for estimation of ERK1/2 phosphorylation by immunobloting.

Cells were stimulated with 100 nM Ang II and 200 μM H_2O_2 for various times with or without pre-treatment of NAC for 30 min. After treatment, cells were washed twice with ice-cold PBS and placed on ice immediately. Cells were lysed with 100 μL SDS sample buffer (50 mM Tris–HCl, 100 mM DTT, 2% SDS, 0.1% BPB, 10% glycerol). Solubilized proteins were quantified by the Lawry method using protein assay kit (Bio-Lad). Proteins (25 μg) were separated on 12.5% polyacrylamide gels using SDS–PAGE and transferred to nitrocellulose membrane at 40 mA for 57 min. Membranes were blocked overnight at 4 with TBS-T containing 5% non-fat dry milk and 0.1% Tween 20. The blots were incubated for overnight at 4 °C with primary antibody (rabbit polyclonal anti-phospho specific ERK1/2 antibody at 1:1000, New England Biolabs; NEB, Boverly, MA) in TBS-T and incubated for 1 h at room temperature with secondary antibody (AP-conjugated gout anti-rabbit antibody at 1:1000, NEB) in same buffer. Phospholylated ERK1 and 2 were visualized with NBT/BCIP solution (Boehringer Mannheim).

2.6. Immunoprecipitation and p38MAPK activity assay

VSMCs were plated and quiescent as described above for estimation of p38MAPK activity assay. Cells were stimulated with agonists at 37 °C in serum free DMEM for specified durations. After treatment, cells were washed twice with ice-cold PBS and placed on ice. Cells were lysed with ice-cold buffer containing 20 mM Tris–HCl pH 7.5, 150 mM NaCl, 1 mM EDTA, 1 mM EGTA, 1% Triton X-100, 2.5 mM sodium pyrophosphate, 1 mM β-glycerolphosphate, 1 mM Na_3VO4, 1 μg/mL leupeptin, protease inhibitor cocktail (Sigma) and sonicated 4 times for 5 s each, on ice. Cell lysates were then centrifuged at 13 000×*g* for 10 min at 4 °C. For immunoprecipitation, 300 μg cell lysates was incubated with anti-p38MAPK antibody (1:50) for overnight at 4 °C with gentle rocking, and then 20 μL of protein G-sepharose beads added and incubated for 3 h at 4 °C with gentle rocking. The beads were washed twice with 500 μL of cell lysis buffer and twice with 500 μL of kinase buffer (25 mM Tris–HCl pH 7.5, 5 mM β-glycerolphosphate, 2 mM DTT, 0.1 mM Na_1VO4, 10 mM MgCl2). For kinase assay, the beads were suspended with 50 μL of kinase buffer supplemented with 200 μM ATP and 2 μg ATF-2 fusion protein, the substrate for p38MAPK, and incubated 30 min at 30 °C. Proteins were separated on 12.5% polyacrylamide gels using SDS–PAGE and transferred to nitrocellulose membrane at 40 mA for 57 min. Membranes were locked overnight at 4 °C with TBS-T. The blots were incubated for overnight at 4 °C with primary antibody (rabbit polyclonal anti-ATF-2 antibody at 1:1000, NEB) in TBS-T and incubated for 1 h at room temperature with secondary antibody (HRP-conjugated gout anti-rabbit antibody at 1:2000, NEB) in same buffer. Phospholylated ATF-2 protein was detected with ECL solution.

2.7. Statistical analysis

All results were expressed as mean±S.D. Statistical analysis of the data was performed using ANOVA. $P<0.05$ was considered to be statistically significant.

3. Results

3.1. Effect of exogenous H_2O_2 and Ang II on intracellular H_2O_2 level

To address the effect of H_2O_2 and Ang II on intracellular H_2O_2 accumulation in VSMCs, we exposed cells to 200 μM H_2O_2 or 100 nM Ang II for 5 min and measured the concentration of DCFH-DA oxidized by H_2O_2 per 1×10^4 cells. Fig. 1 shows H_2O_2- or Ang II-induced representative

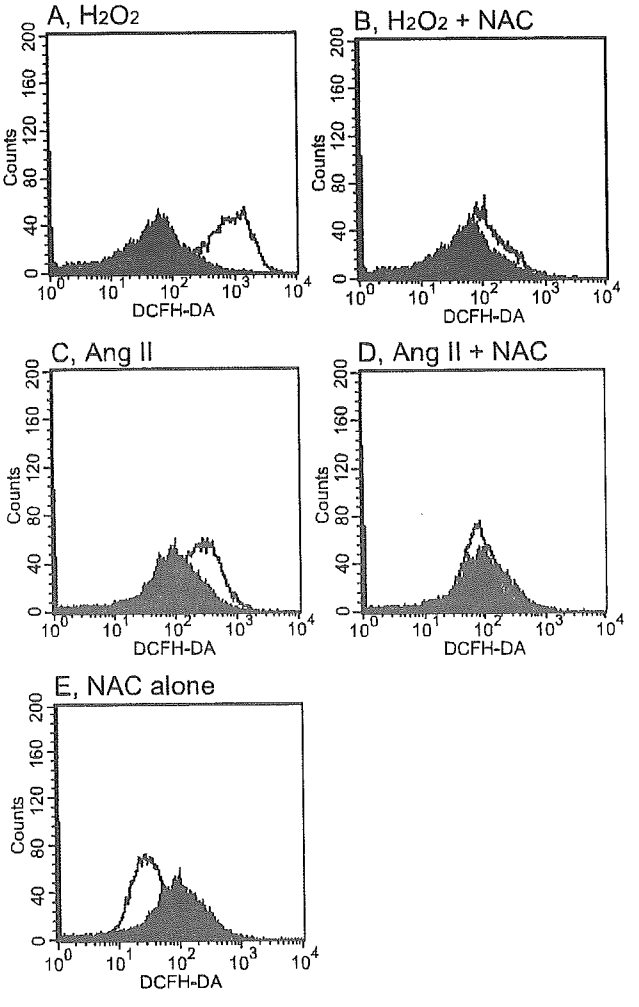

Fig. 1. Change of intracellular H_2O_2 level by Ang II and H_2O_2 treatment in VSMCs. Quiescent VSMCs pretreated with DCF-DA for 10 min were stimulated by 200 M H_2O_2 (A, B), 100 nM Ang II (C, D) or vehicle (E) for 5 min with (B, D, E) or without (A, C) 1 mM NAC pretreatment for 30 min. Then, cells were lysed with Tripsin/EDTA, washed twice with ice-cold PBS and resuspended with ice-cold PBS. The fluorescence intensity of 1×10^4 cells was analysed using a Becton Dickinson FACScan. The experiments were repeated at least two times with similar results.

alteration of intracellular H_2O_2 level in VSMCs as measured by flow cytemetry. As shown in Fig. 1A, exogenous H_2O_2 200 μM remarkably shifted the peak of DCF fluorescence intensity to the right. These effects were almost completely blocked by pre-treatment with 1 mM NAC for 30 min (Fig. 1B). 100 nM Ang II also increased in H_2O_2 concentration (Fig. 1C). Pre-treatment with 1 mM NAC completely inhibited H_2O_2 production by Ang II stimulation (Fig. 1D). Treatment with NAC alone reduced basal production of H_2O_2 (Fig. 1E).

3.2. Effect of Ang II and H_2O_2 on Gax mRNA expression

To determine whether the down-regulation of Gax mRNA expression with Ang II, which we previously reported, is required for oxidative stress, the effect of Ang

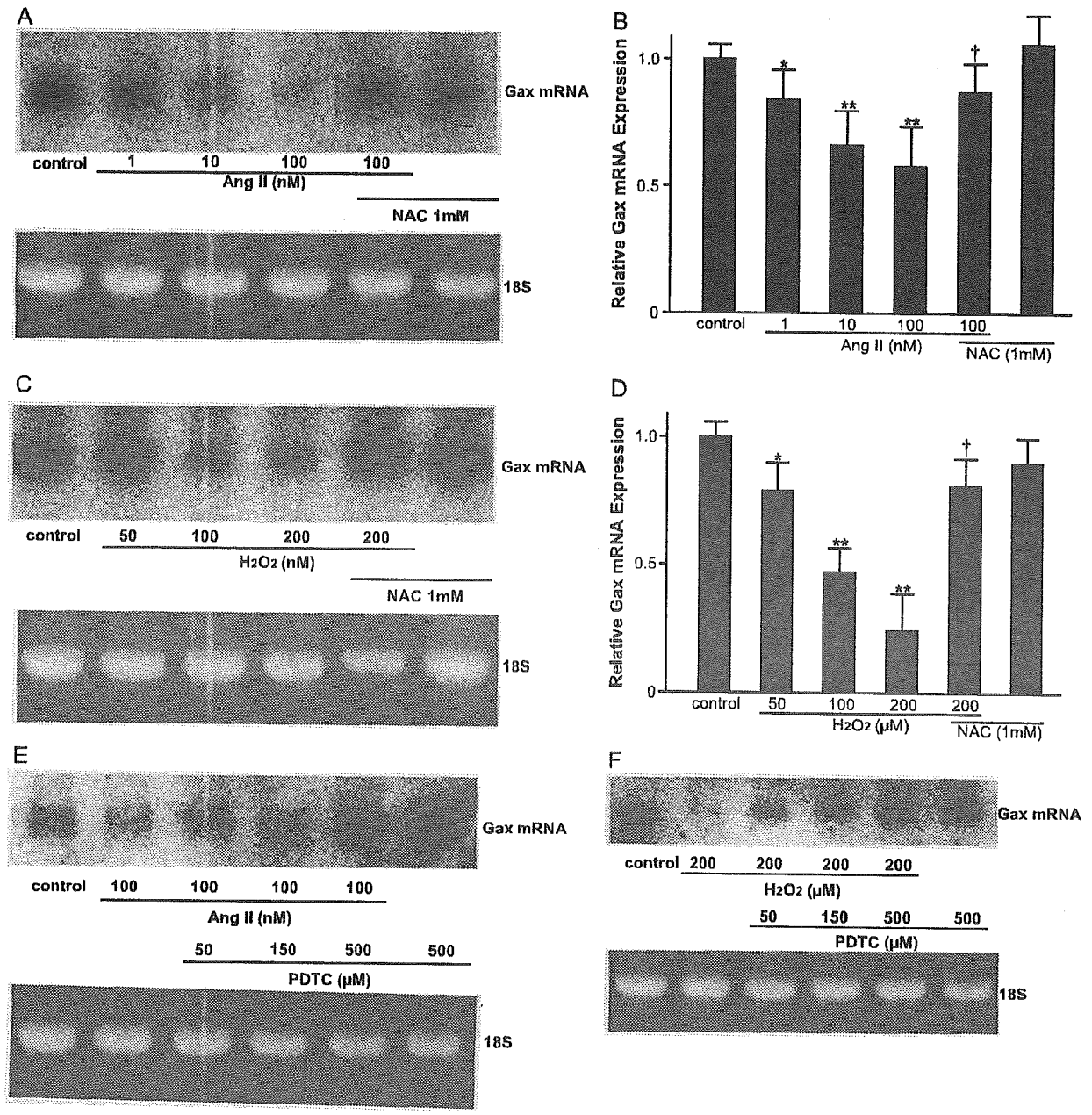

Fig. 2. Dose-dependent effect of Ang II or H_2O_2 on Gax mRNA expression with or without pretreatment of NAC for 30 min. Dose-dependent effect of PDTC on Ang II- or H_2O_2-induced down-regulation of Gax mRNA. (A, C, E, and F) Northern blot analysis for Gax mRNA expression. Quiescent VSMCs were stimulated by vehicle or various concentrations of Ang II for 6 h with or without pretreatment of NAC or PDTC for 30 min and then harvested. Equal aliquots of total RNA (25 g) per lane were applied for the analysis. Lower panel depicts the images of 18S. (B and D) Quantitative measurements of Gax mRNA levels stimulated by Ang II or H_2O_2. The data represent the average percentage of the control. Bars represent the mean±S.D. (n=3). P<0.05, P<0.01 vs. control cells. P<0.05 vs. 100 nM Ang II or 200 M H_2O_2 alone. The experiments for the effects of NAC and PDTC were repeated three times and (n=2 on each), and similar results were obtained.

II and H_2O_2 in the presence or absence of NAC on Gax mRNA expression was examined. As shown in Fig. 2A and B, the administration of Ang II suppressed Gax mRNA expression in a dose-dependent manner. 100 nM Ang II suppressed Gax mRNA expression by about 50% compared with control. The down-regulation of Gax mRNA induced by Ang II was significantly blocked with 1 mM NAC. As shown in Fig. 2C and D, H_2O_2 also suppressed Gax mRNA expression dose-dependently and 200 μM H_2O_2 down-regulated Gax mRNA expression by about 80% compared with control. Pre-treatment with NAC markedly inhibited the down-regulation of Gax mRNA expression induced by H_2O_2. NAC alone has no significant effect on Gax mRNA expression. Moreover, we investigated effects of another antioxidant, PDTC on Ang II- and H_2O_2-induced down-regulation of Gax mRNA in order to delineate the significance of redox-sensitive cascade further. Down-regulation of Gax mRNA expression elicited by Ang II or H_2O_2 was abrogated by PDTC dose-dependently as shown in Fig. 2E and F.

3.3. Effect of Ang II and H_2O_2 on MAPKs phosphorylation

To determine whether the activation of MAPKs induced by Ang II is redox-sensitive or not, we examined the effect of Ang II and H_2O_2 on activation of ERK1/2 and p38MAPK in VSMCs with or without NAC. Fig. 3A shows the time-course of the effect of 100 nM Ang II on ERK1/2 phosphorylation. Rapid and transient phosphorylation of ERK1/2 observed after Ang II stimulation occurred within 5 min and declined 10–30 min after. Pre-treatment with 1 mM NAC potently decreased ERK1/2 phosphorylation elicited with Ang II at 5 min. As shown in Fig. 3B, treatment of 200 μM H_2O_2 also increased ERK1/2 phosphorylation and its activation peaked at 15–20 min and declined in 20–30 min. Pre-treatment of 1 mM NAC also markedly down-regulated H_2O_2-induced ERK1/2 phosphorylation at 20 min similarly.

We also examined the effect of Ang II and H_2O_2 on p38MAPK tyrosine phosphorylation in VSMCs. We could not detect significant phosphorylation of p38MAPK by using the method similar to ERK1/2 measurement. Therefore, we further measured p38MAPK activity using immunoprecipitation (Fig. 3C and D). Ang II and H_2O_2 also slightly activated p38MAPK, and they were blocked by pre-treatment with NAC. However, the level of activated p38MAPK was quite low in comparison with ERK1/2.

3.4. Effect of PD98059 and SB203580 on Ang II-induced down-regulation of Gax mRNA expression

The results presented above demonstrated that Ang II triggered ERK1/2 activation through redox-sensitive signaling in VSMCs. To address the relation of the redox-sensitive MAPK to oxidative stress-induced down-regulation of Gax mRNA expression, we examined the effect of PD98059 and SB203580 on Ang II-induced down-regulation of Gax

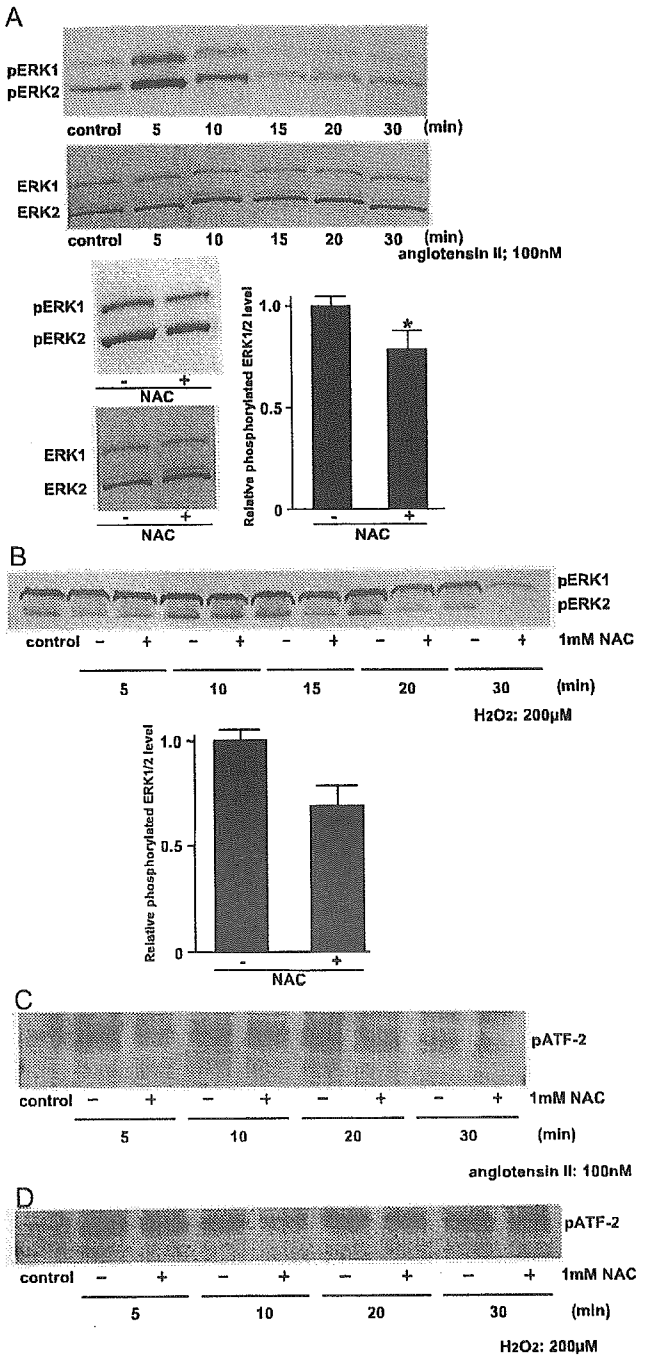

Fig. 3. Effect of Ang II (A) or H_2O_2 (B) on ERK1/2 phosphorylation and effect of NAC on phosphorylated ERK1/2 induced by Ang II or H_2O_2. Quiescent VSMCs were stimulated by 100 nM Ang II or 200 M H_2O_2, respectively, for different time points. NAC was pre-treated for 30 min before administration of Ang II or H_2O_2. Equal aliquots of protein (25 g) from the VSMC lysate were separated by 12.5% SDS–PAGE, followed by immunoblotting for phosphorylated ERK1/2 (pERK1, pERK2). Parallel blots were assayed using the antibodies recognizing the total ERK proteins (ERK1, ERK2). Upper panel represents time-course of ERK1/2 phosphorylation by Ang II or H_2O_2 with or without NAC. Lower panels shows the effect of NAC on the peak level of ERK1/2 phosphorylation induced by Ang II (5 min) or H_2O_2 (20 min). $P<0.01$ vs. control cells. The experiments were repeated four times with similar results. Effect of Ang II (C) or H_2O_2 (D) on ATF-2 phosphorylation and effect of NAC on phosphorylated ATF-2 induced by Ang II or H_2O_2.

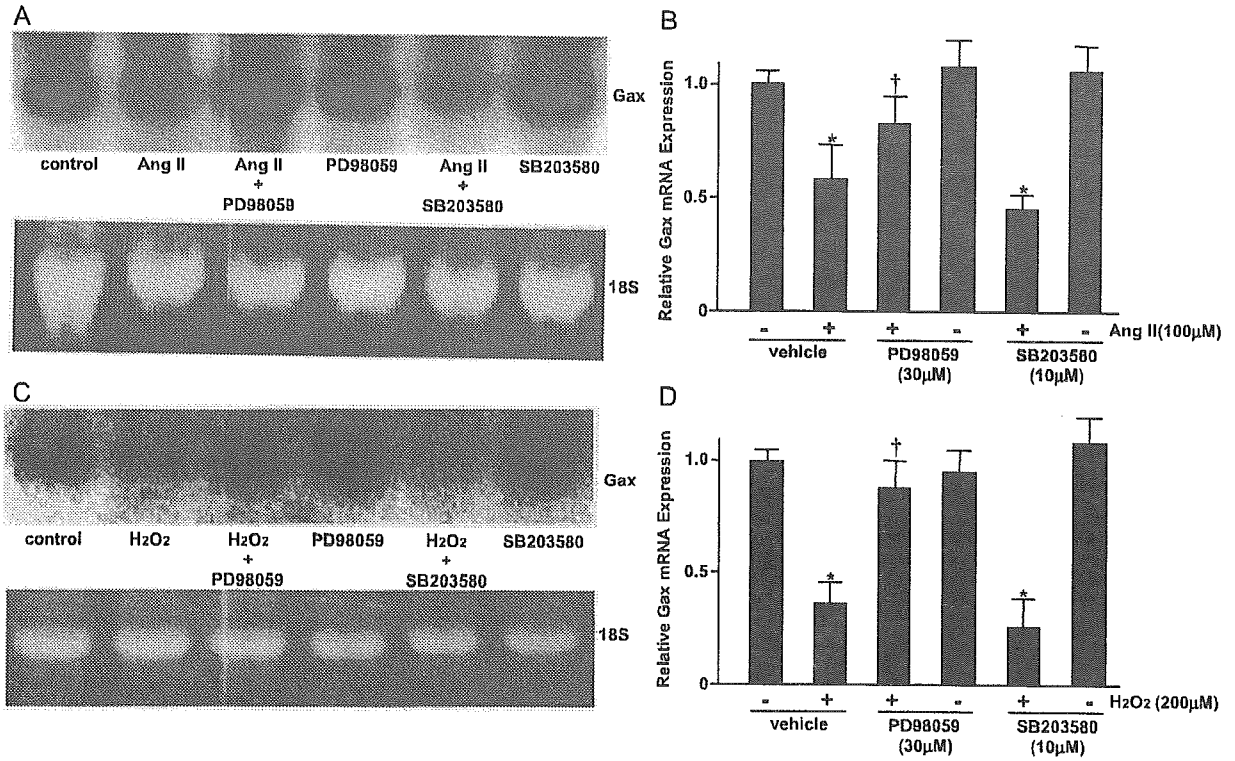

Fig. 4. Effect of PD98059 or SB203580 on Ang II-induced suppression of Gax mRNA expression. (A and C) Northern blot analysis for Gax mRNA expression. Quiescent VSMCs were stimulated by 100 nM Ang II or 200 M H_2O_2 for 6 h with or without pretreatment of PD98059 or SB203580 for 30 min, and then harvested. Equal aliquots of total RNA (25 g) per lane were applied for the analysis. (B and D) Quantitative measurements of Gax mRNA levels stimulated by Ang II or H_2O_2. Bars represent the mean S.D. (n=3). P<0.05, P<0.01 vs. control cells. P<0.05 vs. 100 nM Ang II or 200 M H_2O_2 alone. The experiments were repeated at least three times with similar results.

mRNA expression. As shown in Fig. 4A and B, pretreatment with PD98059 significantly inhibited Ang II-induced down-regulation of Gax mRNA expression by 80% compared with control, while the administration of SB203580 had no effect on Gax expression 6 h after Ang II stimulation. Similarly, PD98059 significantly inhibited H_2O_2-induced down-regulation of Gax mRNA, whereas SB203580 exerted no significant effect.

4. Discussion

In the present study, we demonstrated that Ang II increased intracellular H_2O_2 level and suppressed Gax expression. H_2O_2 mimicked suppressive effect of Ang II on Gax expression. Both Ang II- and H_2O_2-induced down-regulation of Gax expression were blocked by NAC and PDTC. These data indicated that Ang II suppressed Gax expression via increase in intracellular H_2O_2 level. Previously, we reported that down-regulation of Gax expression by Ang II was completely abolished by pretreatment with Ang II type 1 receptor (AT1-R) antagonist, CV11974 [20]. Zafari et al. suggested that Ang II-induced increase in H_2O_2 was inhibited by AT1-R antagonist, losartan [22]. These findings suggest that both the down-regulation of Gax expression and H_2O_2 generation caused by Ang II stimulation were triggered via signaling cascade from AT1-R and imply that H_2O_2 generation mediated via AT1-R activation is involved in Ang II-induced down-regulation of Gax.

It has been reported that Ang II activates three MAPKs, ERK1/2, the c-*jun* NH2-terminal kinases (JNKs, also termed stress-activated protein kinase, SAPK), and p38MAPK in VSMCs [23]. ERK1/2 is rapidly activated in response to virtually all growth factors, leading to a rapid increase in expression of the growth-associated nuclear proto-oncogenes, c-*fos*, c-*jun*, and c-*myc* and recognized to be essential for control of cell growth, division and differentiation in various cells. In contrast, JNK and p38 MAPK are recognized to be activated by environmental stress such as ultraviolet, lipopolysaccharide, hypoxia, osmotic stress, heat shock, and inflammatory cytokines. Recent reports have shown that ERK1/2 and p38MAPK are activated by ROS in VSMCs [12,24]. Therefore, we examined the possible involvement of MAPKs in down-regulation of Gax expression by Ang II or H_2O_2. Both Ang II and H_2O_2 markedly activated ERK1/2 but did not induce p38MAPK phosphorylation significantly. Moreover, down-regulation of Gax by Ang II or H_2O_2 was significantly abrogated by PD98059 administration, while pretreatment with SB203580 had no effect on Gax expression. These results suggest that Ang II or H_2O_2 induce ERK1/2 activation, and down-regulate Gax expression mainly through ERK1/2 activation, indicating that redox-sensitive

ERK1/2 activation is involved in the signaling cascade of Ang II–Gax pathway.

In this study, we demonstrated that Ang II increased in intracellular H_2O_2 concentration within 5 min. As shown in Fig. 3A, in Ang II-induced ERK1/2 activation, the pathway via elevation of intracellular H_2O_2 concentration is considered to exert the effect 5 min after Ang II administration. As for Ang II-induced down-regulation of Gax mRNA as shown in Fig. 4, the pathway via ERK1/2 activation contributed to it by about 50%. In contrast, as shown in Fig. 4D, H_2O_2 suppresses Gax mRNA expression mainly via ERK1/2 activation. Therefore, other pathways besides H_2O_2 pathways are responsible for Ang II-induced down-regulation of Gax mRNA expression.

We demonstrated the transient and rapid phosphorylation of ERK1/2 and increment of H_2O_2 concentration induced by Ang II within 5 min. Moreover, we also showed that slow activation of ERK1/2 in spite of rapid increment of intracellular H_2O_2 concentration induced by exogenous H_2O_2 administration. This discrepancy may suggest that H_2O_2 has a minor role for the peak of Ang II-induced ERK1/2 phospholylation within 5 min, and increment of intracellular H_2O_2 is more related to the late phase of ERK1/2 phospholylation (Fig. 3B). Eguchi and colleagues demonstrated that Ang II-induced MAPK activation could be mediated by p21ras activation through a currently unidentified tyrosine kinase that lies downstream of Gq-coupled Ca2+/calmodulin signals [25]. In fact, as shown in Fig. 3A and B, NAC-induced suppression of ERK1/2 phospholylation was only 20%. We considered that Ang II induced ERK1/2 phospholylation through several signal transductions perhaps including the increment of intracellular H_2O_2 concentration.

Baas et al. demonstrated that Ang II produces superoxide in VSMCs [26]. In the present study, superoxide was certainly produced and would contribute to the results we showed. Superoxide is commonly known to be reduced by superoxide dismutase to H_2O_2, therefore, we consider that Ang II increases intracellular H_2O_2 concentration through superoxide production and causes the effects. Although we did not investigate a specific effect of superoxide, we believe that could sufficiently demonstrate the function of Ang II-induced oxidative stress by examining the effects of H_2O_2 as a metabolite of superoxide and NAC as an antioxidant agent.

Both Ushio-Fukai et al. and Zafari et al. previously showed that oxidative stress rapidly induced by Ang II administration was important for VSMCs growth [12,22,27]. Several reports revealed that suppression of Gax expression was related to growth retardation of VSMCs [14,15,20]. As mentioned above, the present study also supports that oxidative stress induces growth of VSMCs possibly in part via suppression of Gax expression. Ushio-Fukai et al. have shown that only p38MAPK, but not ERK1/2, is activated by H_2O_2 in VSMC and involved in Ang II-induced VSMC hypertrophy [12]. In our study, Ang II induced marked ERK1/2 activation but did not cause significant augmentation of p38MAPK activity, and the former is crucial for down-regulation of Gax expression, although exact reason for the difference is unclear at present, there might be the possibility that the culture condition of the cells is different. The passage and culture medium were identical. When the cells were made quiescent, we performed the experiments without serum, while they did the experiment with 0.1% serum. Furthermore, whereas they administrated agents under the conditions of 80–90% cell density, we performed the experiments with 50–70% cell density.

Recently, Abe et al. have showed that H_2O_2 activates ERK1/2 dose-dependently in bovine tracheal smooth muscle cells [28]. Lee et al. also showed H_2O_2 activated ERK1/2 in a time-dependent fashion in rat lung artery smooth muscle cells and activation of ERK1/2 reached maximal level 20 min later [29]. Moreover, Frank et al. revealed that H_2O_2 induced ERK1/2 activation in VSMCs [30]. These results are compatible with our results. On the other hand, Huot et al. showed that p38MAPK was induced by H_2O_2 [31]. The difference on Ang II-induced p38MAPK is not clear at present.

Previously, Tsai et al. showed NAC and PDTC induce apoptosis in VSMCs [32]. They demonstrated the results using 5 mM NAC, which was considered to be very high. In addition, their experiments were performed in very low cell density condition. It is considered that apoptosis was easily induced in their experimental condition. As mentioned above, we performed all experiments in higher cell density condition compared to their experiments. We did not confirm whether apoptosis was induced by NAC administration, however, we consider that there is little involvement of apoptosis in the present study, since floating cells were not seen in NAC-treated groups and there was no difference in the time amount of RNA harvested from VSMCs with NAC-treated groups and non-treated groups.

In our previous report, we speculated that gene regulation of Gax expression was under control of a molecule commonly used by AT1-R and PDGF receptor signaling pathways because of the similar action of Ang II and PDGF on Gax expression [20]. In this study, it was shown that down-regulation of Gax by Ang II is mediated through redox-sensitive ERK1/2 activation. In another series of our experiment, we have confirmed that PDGF-induced down-regulation of Gax is also remarkably suppressed by treatment with NAC. These findings suggests the existence of redox-sensitive pathway, which induces down-regulation of Gax, after the convergence of AT1-R and PDGF receptor signaling pathways. Sundaresan et al. exhibited that the PDGF-stimulated increase in intracellular H_2O_2 and the effects of PDGF stimulation on ERK1/2 activation, migration, and DNA synthesis were inhibited by infection of VSMCs with an adenovirus that encodes catalase, a specific reductase of H_2O_2 [33]. These evidences and our data indicate the significance of intracellular H_2O_2 accumulation and ERK1/

2 activation in growth-promoting signaling pathway induced by several stimuli, including Ang II and PDGF, and suggest the importance of Gax as a common molecule existed in the redox-sensitive growth control pathway.

In conclusion, we demonstrated that Ang II down-regulated Gax expression via redox-sensitive ERK1/2 activation in VSMCs. This implies the possibility that Gax can be one of the inhibitory molecules in Ang II-induced VSMC hypertrophy via redox-sensitive pathway.

Acknowledgments

We would like to thank Ms. A. Sone, Ms. A. Nonoguchi, and Ms. Y. Takada for their excellent secretarial work. This work was supported in part by research grants from the Japanese Ministry of Education, Science and Culture; Japanese Ministry of Health and Japanese Society for the Promotion of Science 'Research for the Future' program (JSPS-RFTF 96100204, JSPS-RFTF98L00801).

References

[1] Nakazono K, Watanabe N, Matsuno K, Sasaki J, Sato T, Inoue M. Does superoxide underlie the pathogenesis of hypertension? Proc Natl Acad Sci U S A 1991;15, 88(22):10045–8.
[2] de Bono DP, Yang WD. Exposure to low concentrations of hydrogen peroxide causes delayed endothelial cell death and inhibits proliferation of surviving cells. Atherosclerosis 1995;24, 114(2):235–45.
[3] Rao GN, Berk BC. Active oxygen species stimulate vascular smooth muscle cell growth and proto-oncogene expression. Circ Res 1992;70(3):593–9.
[4] Griendling KK, Ushio-Fukai M. Redox control of vascular smooth muscle proliferation. J Lab Clin Med 1998;132(1):9–15.
[5] Bellas RE, Lee JS, Sonenshein GE. Expression of a constitutive NF-kappa B-like activity is essential for proliferation of cultured bovine vascular smooth muscle cells. J Clin Invest 1995;96(5):2521–7.
[6] Schmidt AM, Hori O, Chen JX, Li JF, Crandall J, Zhang J, et al. Advanced glycation endproducts interacting with their endothelial receptor induce expression of vascular cell adhesion molecule-1 (VCAM-1) in cultured human endothelial cells and in mice. A potential mechanism for the accelerated vasculopathy of diabetes. J Clin Invest 1995;96(3):1395–404.
[7] Holvoet P, Vanhaecke J, Janssens S, Van de Werf F, Collen D. Oxidized LDL and malondialdehyde-modified LDL in patients with acute coronary syndromes and stable coronary artery disease. Circulation 1998;13, 98(15):1487–94.
[8] Pollman MJ, Hall JL, Gibbons GH. Determinants of vascular smooth muscle cell apoptosis after balloon angioplasty injury. Influence of redox state and cell phenotype. Circ Res 1999;8–22, 84(1):113–21.
[9] Itoh H, Mukoyama M, Pratt RE, Gibbons GH, Dzau VJ. Multiple autocrine growth factors modulate vascular smooth muscle cell growth response to angiotensin II. J Clin Invest 1993;91(5):2268–74.
[10] Berk BC, Corson MA. Angiotensin II signal transduction in vascular smooth muscle: role of tyrosine kinases. Circ Res 1997;80(5):607–16.
[11] Laursen JB, Rajagopalan S, Galis Z, Tarpey M, Freeman BA, Harrison DG. Role of superoxide in angiotensin II-induced but not catecholamine-induced hypertension. Circulation 1997;95(3):588–93.
[12] Ushio-Fukai M, Alexander RW, Akers M, Griendling KK. p38 Mitogen-activated protein kinase is a critical component of the redox-sensitive signaling pathways activated by angiotensin II. Role in vascular smooth muscle cell hypertrophy. J Biol Chem 1998;12,273 (24):15022–9.
[13] Patterson KD, Cleaver O, Gerber WV, Grow MW, Newman CS, Krieg PA. Homeobox genes in cardiovascular development. Curr Top Dev Biol 1998;40:1–44.
[14] Gorski DH, Le Page DF, Patel CV, Copeland NG, Jenkins NA, Walsh K. Molecular cloning of a diverged homeobox gene that is rapidly down-regulated during the G0/G1 transition in vascular smooth muscle cells. Mol Cell Biol 1993;13(6):3722–33.
[15] Smith RC, Branellec D, Gorski DH, Guo K, Perlman H, Dedieu JF, et al. p21CIP1-mediated inhibition of cell proliferation by over-expression of the gax homeodomain gene. Genes Dev 1997;1, 11(13):1674–89.
[16] Maillard L, Van Belle E, Smith RC, Le Roux A, Denefle P, Steg G, et al. Percutaneous delivery of the gax gene inhibits vessel stenosis in a rabbit model of balloon angioplasty. Cardiovasc Res 1997;35(3):536–46.
[17] Dzau VJ, Gibbons GH. Endothelium and growth factors in vascular remodeling of hypertension. Hypertension 1991;18(Suppl. 5): III115–21.
[18] Itoh H, Pratt RE, Dzau VJ. Atrial natriuretic polypeptide inhibits hypertrophy of vascular smooth muscle cells. J Clin Invest 1990; 86(5):1690–7.
[19] Komatsu Y, Itoh H, Suga S, Ogawa Y, Hama N, Kishimoto I, et al. Regulation of endothelial production of C-type natriuretic peptide in coculture with vascular smooth muscle cells. Role of the vascular natriuretic peptide system in vascular growth inhibition. Circ Res 1996;78(4):606–14.
[20] Yamashita J, Itoh H, Ogawa Y, Tamura N, Takaya K, Igaki T, et al. Opposite regulation of Gax homeobox expression by angiotensin II and C-type natriuretic peptide. Hypertension 1997;29(1 Pt. 2): 381–7.
[21] Lee AC, Fenster BE, Ito H, Takeda K, Bae NS, Hirai T, et al. Ras proteins induce senescence by altering the intracellular levels of reactive oxygen species. J Biol Chem 1999;274(12):7936–40.
[22] Zafari AM, Ushio-Fukai M, Akers M, Yin Q, Shah A, Harrison DG, et al. Role of NADH/NADPH oxidase-derived H_2O_2 in angiotensin II-induced vascular hypertrophy. Hypertension 1998;32(3):488–95.
[23] Takahashi E, Berk BC. MAP kinases and vascular smooth muscle function. Acta Physiol Scand 1998;164(4):611–21.
[24] Chakraborti S, Chakraborti T. Oxidant-mediated activation of mitogen-activated protein kinases and nuclear transcription factors in the cardiovascular system: a brief overview. Cell Signal 1998;10 (10):675–83.
[25] Eguchi S, Matsumoto T, Motley ED, Utsunomiya H, Inagami T. Identification of an essential signaling cascade for mitogen-activated protein kinase activation by angiotensin II in cultured vascular smooth muscle cells. J Biol Chem 1996;271(24):14169–75.
[26] Baas AS, Berk BC. Differential activation of mitogen-activated protein kinases by H_2O_2 and O2-in vascular smooth muscle cells. Circ Res 1995;77(1):29–36.
[27] Zafari AM, Ushio-Fukai M, Minieri CA, Akers M, Lassegue B, Griedling KK. Arachidonic acid metabolites mediate angiotensin II-induced NADH/NADPH oxidase activity and hypertrophy in vascular smooth muscle cells. Antioxid Redox Signal 1999;1(2): 167–79.
[28] Abe MK, Kartha S, Karpova AY, Li J, Liu PT, Kuo WL, et al. Hydrogen peroxide activates extracellular signal-regulated kinase via protein kinase C, Raf-1, and MEK1. Am J Respir Cell Mol Biol 1998;18:562–9.
[29] Lee SL, Simon AR, Wang WW, Fanburg BL. H_2O_2 signals 5-HT-induced ERK MAP kinase activation and mitogenesis of smooth muscle cells. Am J Physiol, Lung Cell Mol Physiol 2001;281:L646–52.
[30] Frank GD, Eguchi S, Inagami T, Motley ED. *N*-acetylcycteine inhibits angiotensin II-mediated activation of extracellular signal-regulated kinase and epidermal growth factor receptor. Biochem Biophys Res Commun 2001;280(4):1116–9.

[31] Huot J, Houle F, Marceau F, Landry J. Oxidative stress-induced actin reorganization mediated by the p38mitogen-activated protein kinase/heat shock protein 27 pathway in vascular endothelial cells. Circ Res 1997;80(3):383–92.
[32] Tsai JC, Jain M, Hsieh CM, Lee WS, Yoshimizu M, Patterson C, et al. Induction of apoptosos by pyrrolidinedithiocarbamate and *N*-acetylcysteine in vascular smooth muscle cells. J Biol Chem 1996;271(7):3667–70.
[33] Sundaresan M, Yu ZX, Ferrans VJ, Irani K, Finkel T. Requirement for generation of H_2O_2 for platelet-derived growth factor signal transduction. Science 1995;270(5234):296–9.

The PTEN/PI3K pathway governs normal vascular development and tumor angiogenesis

Koichi Hamada,[1] Takehiko Sasaki,[2] Pandelakis A. Koni,[4] Miyuki Natsui,[1] Hiroyuki Kishimoto,[1] Junko Sasaki,[1,2] Nobuyuki Yajima,[1] Yasuo Horie,[1,3] Go Hasegawa,[5] Makoto Naito,[5] Jun-ichi Miyazaki,[6] Toshio Suda,[7] Hiroshi Itoh,[8] Kazuwa Nakao,[8] Tak Wah Mak,[9,11] Toru Nakano,[10,11] and Akira Suzuki[1,11,12]

[1]Department of Molecular Biology, [2]Department of Microbiology, [3]Department of Gastroenterology, Akita University School of Medicine, Akita 010-8543, Japan; [4]Molecular Immunology Program, Institute of Molecular Medicine and Genetics, Medical College of Georgia, Augusta, Georgia 30912, USA; [5]Department of Cellular Function, Niigata University Graduate School of Medical and Dental Sciences, Niigata 951-8510, Japan; [6]Division of Stem Cell Regulation Research, Osaka University Graduate School of Medicine, Suita 565-0871, Japan; [7]Department of Cell Differentiation, The Sakaguchi Laboratory, School of Medicine, Keio University School of Medicine, Tokyo 160-8582, Japan; [8]Department of Medicine and Clinical Science, Kyoto University Graduate School of Medicine, Kyoto 606-8507, Japan; [9]The Campbell Family Institute of Breast Cancer Research, and Departments of Immunology and Medical Biophysics, University of Toronto, Toronto M5G 2C1, Ontario, Canada; [10]Department of Pathology, Medical School and Graduate School of Frontier Biosciences, Osaka University, Suita 565-0871, Japan

***PTEN* is an important tumor suppressor gene. Hereditary mutation of *PTEN* causes tumor-susceptibility diseases such as Cowden disease. We used the *Cre-loxP* system to generate an endothelial cell-specific mutation of Pten (*Tie2CrePten*) in mice. *Tie2CrePten*$^{flox/+}$ mice displayed enhanced tumorigenesis due to an increase in angiogenesis driven by vascular growth factors. This effect was partially dependent on the PI3K subunits *p85*α and *p110*γ. In vitro, *Tie2CrePten*$^{flox/+}$ endothelial cells showed enhanced proliferation/migration. *Tie2CrePten*$^{flox/flox}$ mice died before embryonic day 11.5 (E11.5) due to bleeding and cardiac failure caused by impaired recruitment of pericytes and vascular smooth muscle cells to blood vessels, and of cardiomyocytes to the endocardium. These phenotypes depend strongly on *p110*γ rather than on *p85*α and were associated with decreased expression of Ang-1, VCAM-1, connexin 40, and ephrinB2 but increased expression of Ang-2, VEGF-A, VEGFR1, and VEGFR2. Pten is thus indispensable for normal cardiovascular morphogenesis and post-natal angiogenesis, including tumor angiogenesis.**

[*Keywords*: PTEN; PI3K; endothelial cells; cardiovasculogenesis; tumor angiogenesis]

Supplemental material is available at http://www.genesdev.org.

Received February 22, 2005; revised version accepted June 27, 2005.

PTEN is a tumor suppressor gene (Li et al. 1997) that is mutated in many human sporadic cancers and in hereditary tumor susceptibility disorders such as Cowden disease (Liaw et al. 1997). PTEN is a multifunctional phosphatase whose major substrate is phosphatidylinositol-3,4,5-trisphosphate (PIP3) (Maehama and Dixon 1998), a lipid second messenger molecule. PIP3 activates numerous downstream targets, including the serine–threonine kinase PKB/Akt, which is involved in anti-apoptosis, proliferation, and oncogenesis (Gerber et al. 1998). By using its lipid phosphatase activity to dephosphorylate PIP3, PTEN negatively regulates the phosphoinositide-3-kinase (PI3K)–PKB/Akt pathway and thus exerts tumor suppression. PI3K family members are classified into three groups according to their structures and substrate specificities. Among them, class I PI3Ks produce PIP3 and are involved in receptor-mediated signaling. Class I PI3Ks are further divided into two subclasses. Class IA heterodimeric PI3Ks, consisting of a catalytic subunit (*p110*α, *p110*β, *p110*δ) and a regulatory subunit (*p85*α, *p85*β, *p55*γ), are involved in receptor tyrosine kinase (RTK) pathways, whereas class IB PI3K (*p110*γ) acts downstream of G-protein-coupled receptors (GPCRs). Both classes of PI3Ks can be activated by a wide range of vascular growth factors (VGFs).

Embryonic cardiovascular development and post-natal neovascularization (including tumor angiogenesis) are

[11]**These authors contributed equally to this work.**
[12]**Corresponding author.**
E-MAIL suzuki@med.akita-u.ac.jp; FAX 81-18-884-6077.
Article published online ahead of print. Article and publication date are at http://www.genesdev.org/cgi/doi/10.1101/gad.1308805.

complex processes that share signaling molecules (Daniel and Abrahamson 2000). These processes depend on shear stress and coordinated interactions between endothelial VGFs (e.g., VEGF, Ang-1, Ang-2, *b*FGF, PDGF-B, ephrin-B2, TGF-β superfamily members), intracellular signaling molecules (e.g., Notch1, COUP-TFII), and intercellular contacts (e.g., connexins, VCAM-1). Mutations of these molecules cause defects in cardiovascular development (Dickson et al. 1995; Suri et al. 1996; Lindahl et al. 1997; Larsson et al. 2001; Lindblom et al. 2003). Significantly, all of the above growth factors also activate the PI3K–PKB/Akt pathway.

Normal cardiovascular development requires communication between endothelial cells and surrounding mesenchymal cells (Suri et al. 1996; Hellstrom et al. 2001). The vascular wall is composed of endothelial cells that surround the lumen of the vessel, backed by layers of pericytes (PCs) in microvessels, or vascular smooth muscle cells (vSMCs) in large vessels (Hungerford and Little 1999). Cross-talk between endothelial cells and PCs or vSMCs is critical for vascular remodeling and maturation. Defects in PC/vSMC recruitment, such as result from mutations abrogating signaling via PDGF-B (Lindahl et al. 1997), Ang-1 (Suri et al. 1996), or TGF-β (Dickson et al. 1995), result in vascular abnormalities.

PTEN is important for normal cardiovascular homeostasis. In vitro, PTEN inhibits vascular sprouting and endothelial tube formation induced by VEGF; dominant-negative mutation of *PTEN* abolishes these effects (Huang and Kontos 2002). Su et al. (2003) have shown that tumor angiogenesis and tumor growth in vivo are blocked by Pten overexpression in tumor cells or by administration of PI3K inhibitors. However, it was not clear in that study whether the inhibition of tumor growth was caused by the angiogenesis defect or by a direct effect on the tumor cells. Here we demonstrate that the role of PTEN in cardiovasculogenesis and angiogenesis is to regulate the expression of vascular signaling molecules, particularly VGFs.

Results

Generation of endothelial cell-specific Pten*-deficient mice*

We generated a conditional *Pten* knockout mouse in which Pten expression was governed by *Tie2*, an endothelial cell-specific promoter. *Pten* exon 5, which encodes the phosphatase domain, was flanked with *loxP* sequences (*Ptenflox*) (Fig. 1A; Suzuki et al. 2001). $Pten^{flox/flox}$ males were crossed with $Pten^{flox/+}$ females that carried a single *Tie2Cre* transgenic locus (Koni et al. 2001) coupled to a reporter transgene (CAG–loxP–CAT–loxP–EGFP) (Kawamoto et al. 2000). Analysis of reporter-positive *Tie2Cre* progeny showed that recombination occurred mainly in endocardial cells and systemic endothelial cells but not in PCs/vSMCs (Fig. 1B). PCR examination of DNA from embryonic day 9.5 (E9.5) cells positive for the endothelial cell marker VEGFR2 confirmed that efficient Cre-mediated recombination had occurred in the $Tie2CrePten^{flox/flox}$ mice. Quantitation of recombination was established in preliminary PCR experiments using mixtures of various ratios of $Pten^{\Delta}$ and $Pten^{flox}$ plasmid DNAs under identical PCR conditions (Fig. 1C). The recombination frequency in $VEGFR2^{+}$ cells of $Tie2CrePten^{flox/flox}$ mice was ~95% (Fig. 1D).

Increased angiogenesis and accelerated tumor growth in $Tie2CrePten^{flox/+}$ *mice*

Histological analyses of systemic vessels and the heart revealed no significant structural differences between $Tie2CrePten^{+/+}$ and $Tie2CrePten^{flox/+}$ mice (data not shown). Since VGFs activate the PI3K–PKB/Akt pathway, we investigated whether VGF-stimulated angiogenesis was increased in $Tie2CrePten^{flox/+}$ mice. Matrigel implants impregnated with *b*FGF, *b*FGF + VEGF, *b*FGF + Ang-1, or PBS were administered subcutaneously to $Tie2CrePten^{+/+}$ and $Tie2CrePten^{flox/+}$ mice. Blood vessel infiltration of the implants was quantified by immunostaining with

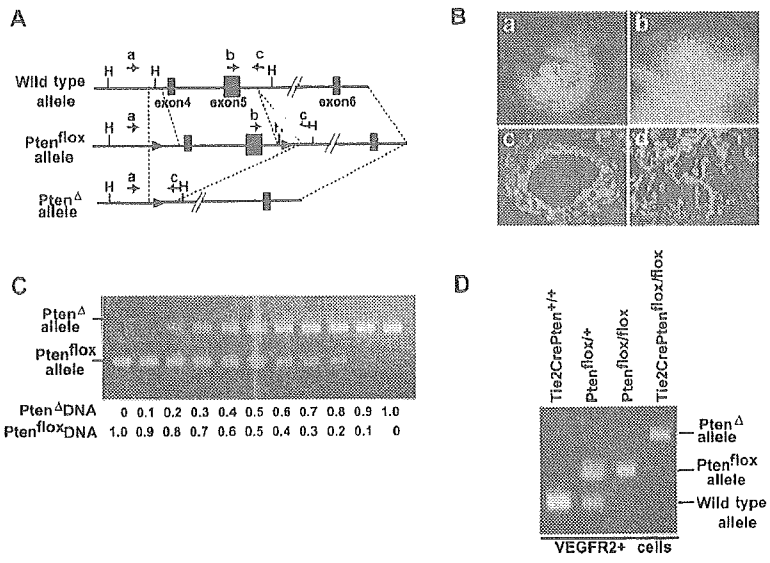

Figure 1. Generation of endothelial cell-specific Pten-deficient ($Tie2CrePten^{flox/flox}$) mice. (*A*) Targeting strategy. Exons of the murine *Pten* gene are represented by ■, and *loxP* sites are indicated by black arrowheads. The floxed ($Pten^{flox}$) and deleted ($Pten^{\Delta}$) alleles are shown. Primers used for genotyping are shown as red arrows (a–c). (*B*) Tissue distribution of *Tie2Cre*-mediated recombination. Immunohistochemistry was used to evaluate GFP expression at E9.5 (panels *a*,*b*), and GFP plus SMA (red) expression in the dorsal aorta (panel *c*) and heart (panel *d*) at E10.5, in *Tie2Cre* Tg mice carrying the reporter transgene. (*C*) Quantitation of genomic PCR. A total of 1 fg of a mixture of various ratios of $Pten^{\Delta}$ and $Pten^{flox}$ plasmid DNAs was used as template DNA. (*D*) Deletion of the *Pten* gene. Genomic PCR of DNA from $VEGFR2^{+}$ cells in E9.5 embryos of the indicated genotype. In $Tie2CrePten^{flox/flox}$ mice, the vast majority of $VEGFR2^{+}$ cells showed deletion of the *Pten* gene. PCR conditions were identical to those in *C*.

anti-CD31 antibody. In contrast to implanted *Tie2CrePten*$^{+/+}$ mice, implanted *Tie2CrePten*$^{flox/+}$ mice showed increased vascularization, even in PBS controls (Fig. 2A). Moreover, angiogenic responses to VGFs were significantly elevated in the mutants (Fig. 2A,B).

To determine whether heterozygous *Pten* deficiency in endothelial cells affected adult tumor angiogenesis, *Tie2CrePten*$^{flox/+}$ and *Tie2CrePten*$^{+/+}$ mice were injected subcutaneously with either melanoma (B16BL6) or Lewis lung carcinoma (LLC) cells. Both cell lines induced significantly larger tumors in *Tie2CrePten*$^{flox/+}$ mice than in *Tie2CrePten*$^{+/+}$ mice (Fig. 2C [top], D). When tumor sections were immunostained with anti-CD31, microvessels were evident in tumors from both *Tie2CrePten*$^{+/+}$ and *Tie2CrePten*$^{flox/+}$ mice, but were more abundant and of larger size in the latter (Fig. 2C [bottom], E). Vessel density in nontumorous adult skin was comparable between *Tie2CrePten*$^{flox/+}$ and *Tie2CrePten*$^{+/+}$ mice (Supplementary Fig. 1A,B).

We next used PCNA staining and the Transwell system to evaluate the proliferation and migration, respectively, of mouse lung endothelial cells (MLECs) from 10-wk-old *Tie2CrePten*$^{+/+}$ and *Tie2CrePten*$^{flox/+}$ mice. In response to stimulation with Ang-1 or VEGF-A, total numbers of PCNA$^+$ cells and their migration were significantly increased in *Tie2CrePten*$^{flox/+}$ cultures compared with controls (Fig. 2F).

Because Tie2 is expressed in hemangioblasts as well as in endothelial cells, *Tie2Cre* also deletes the *Pten* gene in hematopoietic cells. However, numbers and subsets of T cells, NK cells, and NKT cells were all normal in *Tie2CrePten*$^{flox/+}$ mice (Supplementary Fig. 2A,B). *Tie2CrePten*$^{flox/+}$ splenocytes stimulated with either IL-12 or anti-CD3 plus anti-CD28 showed normal IFN-γ secretion (Supplementary Fig. 2C). Because macrophages are crucial for pathological angiogenesis (Bingle et al. 2002), we repeated the above Matrigel and tumor cell implantation experiments using *LysMCrePten*$^{flox/+}$ mice. In these mutant animals, the *Pten* gene is heterozygously deleted in >80% of peritoneal macrophages (data not shown). No differences in tumor angiogenesis were observed between the *LysMCrePten*$^{+/+}$ *and* *LysMCrePten*$^{flox/+}$ genotypes (Supplementary Fig. 2D–F). Thus, the accelerated tumor growth in *Tie2CrePten*$^{flox/+}$ mice results from enhanced angiogenesis driven by increased endothelial cell proliferation/migration and not from defects in macrophages or tumor immunosurveillance.

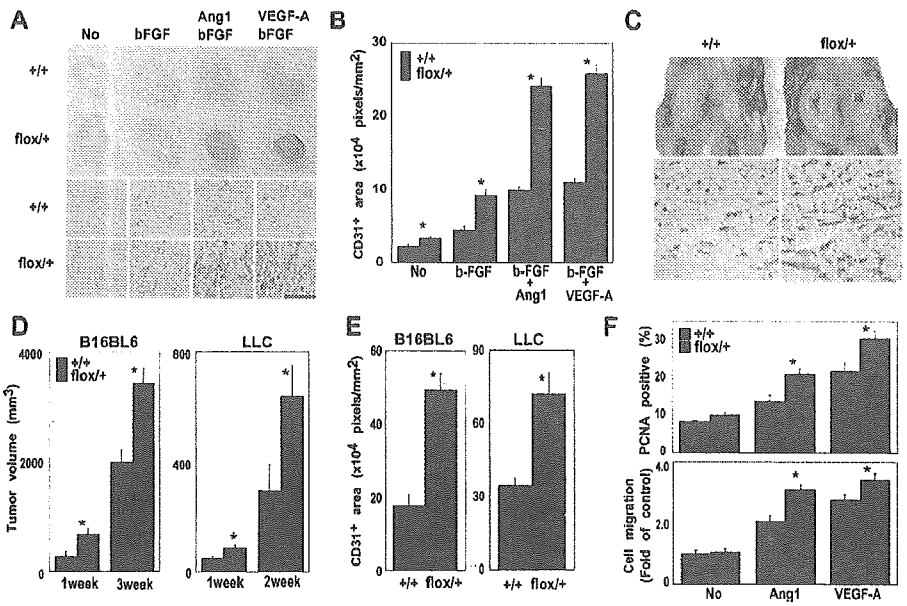

Figure 2. *Tie2CrePten*$^{flox/+}$ mice show increased angiogenesis and accelerated tumor growth. (*A,B*) Increased angiogenesis in response to VGFs. (*A, top*) Representative photos of Matrigel plugs containing no growth factors (No), *b*FGF, *b*FGF + Ang-1, or *b*FGF + VEGF-A. Plugs were removed from *Tie2CrePten*$^{+/+}$ (+/+) and *Tie2CrePten*$^{flox/+}$ (flox/+) mice at 14 d post-injection. Plug vascularization is accelerated in the mutant. (*Bottom*) Anti-CD31 staining of sections of the Matrigel plugs in the *top* panel. Numbers of endothelial cells and vessel structures are increased in the mutant. (*B*) Quantitated vascularization of Matrigel plugs. The area of a plug staining positively with anti-CD31 was quantitated using NIH image software. Significant (*) increases in plug vascularization in response to VGFs were observed in *Tie2CrePten*$^{flox/+}$ mice (flox/+; $n = 8$) compared with wild-type littermates ($n = 8$). (*C–E*) Increased tumor growth. (*C, top*) Representative photos of LCC cells at 2 wk post-implantation in *Tie2CrePten*$^{+/+}$ and *Tie2CrePten*$^{flox/+}$ mice. (*Bottom*) Anti-CD31 staining of sections of the tumors in the *top* panels, showing an increased number of endothelial cells and vessel structures in the mutant. (*D*) Tumor volumes 1–3 wk after transplantation of B16BL6 melanomas ($n = 4$ mice/genotype) or LLC cells ($n = 6$ mice/genotype). (*E*) Quantitation of tumor vascularization 2 wk after implantation of tumor cells in *D*. (*F*) Enhanced proliferation and migration of *Tie2CrePten*$^{flox/+}$ MLECs after stimulation by Ang-1 or VEGF-A. (*Top*) Proliferation of VGF-stimulated MLECs as measured by PCNA immunostaining. (*Bottom*) Migration of MLECs cultured in Transwell cultures for 4 h in the presence of the indicated VGF. For *B*, *D*, *E*, and *F*, results are expressed as the mean ± SEM and are representative of three trials. Statistical differences were determined using the Student's *t*-test; (*) $p < 0.05$.

Death of Tie2CrePten$^{flox/flox}$ *mice by E11.5 due to cardiac failure and bleeding*

The life expectancy, fertility, and gross appearance of viable F1 and F2 *Tie2CrePten$^{flox/+}$* mice appeared normal, but no *Tie2CrePten$^{flox/flox}$* mice were found among 108 offspring from *Tie2CrePten$^{flox/+}$* and *Pten$^{flox/flox}$* intercrosses. Genotyping of 230 progeny of these intercrosses at various embryonic stages showed that homozygous mutant embryos were present at the expected Mendelian frequency up to E9.5, but that resorption commenced at E10.5 and embryonic loss occurred at E11.5 (Table 1).

Histologically, E8.25 *Tie2CrePten$^{flox/flox}$* embryos were essentially normal with respect to gross appearance of the central vascular tree (Fig. 3A, panels a,b), including the rostral-caudal aorta (red arrows), and the anterior and posterior cardiac veins (Fig. 3A, panels c–f, blue arrows). Pten is thus dispensable for the differentiation of angioblasts from the ventral mesoderm, their appropriate migration within the embryo, and their alignment to form major vessels. However, most E8.25 homozygous mutants exhibited delayed heart looping (Fig. 3A, panels g,h, yellow arrows) and enlarged and partially fused yolk sac vessels (Fig. 3A, panels i,j; green arrow). By E9.0, the mutant allantois had connected normally to the chorion (Fig. 3B), but by E9.5, the capillary plexus was enlarged (Fig. 3C, panels a,b, yellow arrows) and distinct branches of large vessels such as the anterior cardinal vein were not formed (Fig. 3C, panels c,d, red arrow) because of a failure in primary vascular plexus remodeling. Vascular sprouting into the neural tube was barely detectable (Fig. 3C, panels e,f, blue arrow). *Tie2CrePten$^{flox/flox}$* embryos also failed to generate distinct vitelline vessels in the yolk sac (Fig. 3D, panels a–d), showing instead a meshwork of interconnected, oversized endothelial cell-lined tubes (Fig. 3D, panels e,f). Dilated capillary-plexus vessels filled the intercapillary spaces (Fig. 3D, panels g,h).

Growth retardation was observed in 50% of E9.5 *Tie2CrePten$^{flox/flox}$* embryos. By E10.5, the majority of mutants showed profound growth retardation as well as pericardial cavity enlargement and frequent bleeding into the pericardial cavity (Fig. 3E, panels a–f, red arrows) or large trunk vessels (Fig. 3E, panel g, blue arrows). Numbers of primitive hematopoietic cells in *Tie2CrePten$^{flox/flox}$* blood vessels were normal from E8.25 to E10.5 (data not shown).

Morphometric analyses showed that vessels in *Tie2CrePten$^{flox/flox}$* yolk sacs were fewer in number (Supplementary Fig. 3A) but larger in diameter (Supplementary Fig. 3B) than in controls. *Tie2CrePten$^{flox/flox}$* yolk sacs also showed an increase in endothelial cell numbers (Supplementary Fig. 3C) that was attributable to proliferation, as judged by their increased staining for Ki67, a nuclear protein highly expressed in proliferating cells (Supplementary Fig. 3D). TUNEL assays revealed no significant differences in numbers of apoptotic endothelial cells in mutant and wild-type yolk sacs (data not shown). No vascular abnormalities were evident in E8.5–E11.5 *Tie2CrePten$^{flox/+}$* embryos. Thus, enhanced endothelial cell proliferation and impaired vascular remodeling are likely responsible for the lethal vascular phenotype of *Tie2CrePten$^{flox/flox}$* embryos.

Impaired recruitment of PCs and vSMCs and defective cardiac muscle development in Tie2CrePten$^{flox/flox}$ *mice*

We examined PC and vSMC recruitment using immunostaining with anti-smooth muscle antigen antibody (αSMA). At E10.0, αSMA$^+$ cells were observed in perivascular regions of the *Tie2CrePten$^{+/+}$* yolk sac (Fig. 3F, panel a) and in the placental extraembryonic circulation (data not shown). In contrast, no αSMA$^+$ PCs/vSMCs were observed adjacent to endothelial cells in *Tie2CrePten$^{flox/flox}$* vessels either in the yolk sac (Fig. 3F, panel b) or placenta (data not shown). In the embryo proper, αSMA staining observed in the vessels, heart, and dorsal aorta of wild-type embryos (Fig. 3F, panels c,e) was dramatically reduced in *Tie2CrePten$^{flox/flox}$* embryos (Fig. 3F, panels d,f). Electron micrographs of E9.5 *Tie2CrePten$^{flox/flox}$* yolk sacs and placenta confirmed the absence of PCs around the capillary network endothelium (Fig. 3F, panel h). The observed bleeding from the large trunk vessels may result from the impaired recruitment of PCs/vSMCs to these tissues. A reduction in the size of the developing intraventricular septum and cardiac trabeculae, and a thinning of the cardiac wall (Fig. 3F, panel f), were also observed in homozygous mutants. The thinnest cardiac walls resembled membranes (Fig. 3F, panel f, blue arrow) such that bleeding in the mutant pericardial cavity could have resulted from cardiac wall rupture or leakage of blood cells from the cardiac lumen. Because

Table 1. *Genotyping of mice derived from* Tie2CrePten$^{flox/+}$ *female and* Pten$^{flox/flox}$ *male intercrosses*

Age (days)	Number of genotypes				No. resorbed embryos[a]
	Pten$^{flox/+}$	*Pten$^{flox/flox}$*	*Tie2CrePten$^{flox/+}$*	*Tie2CrePten$^{flox/flox}$*	
E9.5	25	19	18	20 (15)	0
E10.5	24	25	21	16 (16)	7
E11.5	18	12	13	0	12
P0	13	15	13	0	
P21–28	25	21	21	0	

Genotypes of mice at indicated post-natal (P) or embryonic (E) days were determined using PCR analysis. Numbers in parentheses indicate the total number of abnormal *Tie2CrePten$^{flox/flox}$* embryos counted under a microscope.
[a]Embryos could not be genotyped because of resorption.

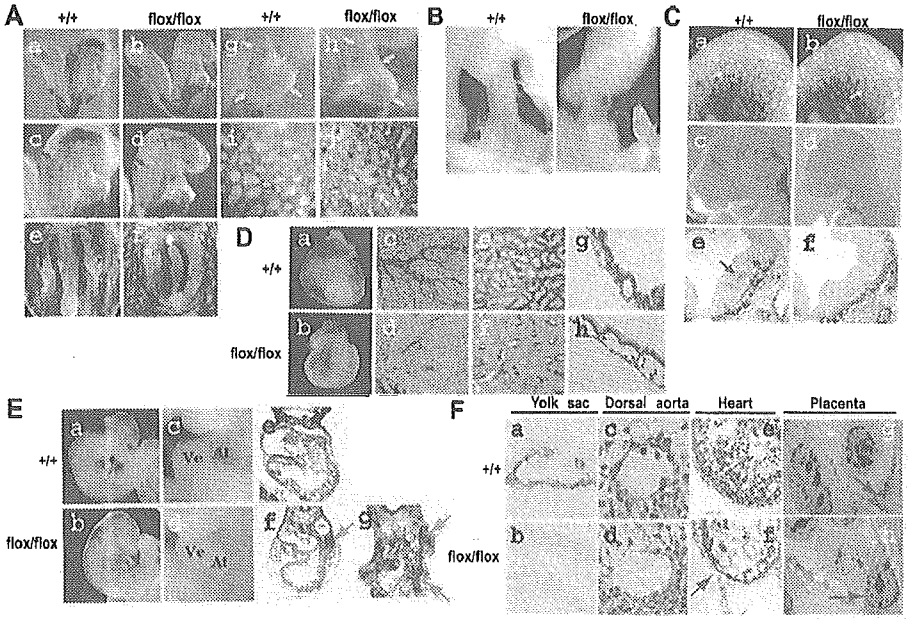

Figure 3. Cardiovascular defects in *Tie2CrePten*$^{flox/flox}$ embryos. (*A*) Whole mounts of E8.25 embryos immunostained with anti-CD31. (Panels *a–f*) Vascular tree components, including the rostral-caudal aorta (red arrows) and anterior and posterior cardiac veins (blue arrows), were grossly normal in *Tie2CrePten*$^{flox/flox}$ embryos. (Panels *g–j*) Delayed heart looping (yellow arrows) and enlarged and partially fused yolk sac vessels (green arrow) were apparent in the mutant. (*B*) Normal chorioallantoic fusion in E9.0 *Tie2CrePten*$^{flox/flox}$ embryos. (*C*) Gross abnormalities in E9.5 *Tie2CrePten*$^{flox/flox}$ embryos. Anti-CD31 staining of whole-mount (panels *a,b*), gross whole-mount (panels *c,d*), and histological LacZ staining (panels *e,f*) of E9.5 embryos are shown for *Tie2CrePten*$^{+/+}$ and *Tie2CrePten*$^{flox/flox}$ embryos carrying the Flk-1$^{+/-}$/LacZ transgene. The mutant shows an enlarged capillary plexus (yellow arrows; panels *a,b*), a failure to remodel distinct branches of the anterior cardinal vein (red arrow; panel *c*), and impaired vascular sprouting into the neural tube (*bottom*, blue arrow; panel *e*). (*D*) Abnormalities in the E9.5 yolk sac. Whole mounts of E9.5 yolk sac (panels *a,b*), and anti-CD31 staining of yolk sac tissues (panels *c–f*), and H&E staining of yolk sac tissues (panels *g,h*) are shown. (Panels *a–d*) A failure of vascular remodeling to form mature distinct vitelline vessels can be clearly seen in the homozygous mutant yolk sac. (Panels *e–h*) Interconnected and homogeneously dilated endothelial cell-lined tubes are present. (*E*) Fatal cardiovascular abnormalities. E10.5 *Tie2CrePten*$^{flox/flox}$ embryos showed an enlarged pericardial cavity, and frequent bleeding (red arrows) in the cavity (panels *b,d,f*) or in large trunk vessels (panel *g*). Panels *e–g* show H&E staining. (At) Atrium; (Ve) ventricle. (*F*) Decreased α-SMA expression in mutant embryonic vasculature (panels *a–d*) and heart (panels *e,f*). In E10.0 *Tie2CrePten*$^{+/+}$ embryos, perivascular walls in both the yolk sac (panel *a*) and dorsal aorta (panel *c*) are lined with α-SMA$^+$ PCs/vSMCs. (Panels *b,d*) αSMA expression is dramatically reduced in E10.0 *Tie2CrePten*$^{flox/flox}$ embryos. (Panels *e,f*) Reductions in the sizes of αSMA$^+$ cardiac muscle walls, the intraventricular septum, and cardiac trabeculae were also observed in *Tie2CrePten*$^{flox/flox}$ heart. (Panels *g,h*) Electron micrographs of E9.5 placentae reveal an absence of pericytes around the capillary network endothelium. (Blue arrows) Endothelial cells; (yellow arrows) blood cells in the vessel; (red arrows) pericytes.

the *Tie2CrePten*$^{flox/flox}$ vascular phenotype precedes the development of a functional circulation and the onset of growth retardation, these defects are most likely due to the *Pten* mutation and are not secondary to circulatory failure, ischemia, or growth retardation.

Altered expression of VGFs in Tie2CrePten$^{+/+}$ *and* Tie2CrePten$^{flox/flox}$ *mice*

RT–PCR analyses of gene expression in whole yolk sacs from E8.5 *Tie2CrePten*$^{+/+}$ *and Tie2CrePten*$^{flox/flox}$ embryos showed that a lack of Pten significantly reduced expression of connexin-40, Ang-1, ephrinB2, and VCAM-1, but increased expression of Ang-2, VEGF-A, VEGFR1, VEGFR2, TGF-β1, and PAI-1 (Fig. 4A). These differences were confirmed by RT–PCR analyses of VEGFR2$^+$ cells from E9.5 *Tie2CrePten*$^{+/+}$ and *Tie2CrePten*$^{flox/flox}$ embryos (Fig. 4B), and by RT–PCR (Fig. 4C) and protein (Fig. 4D,E) analyses of human umbilical vein endothelial cells (HUVECs) in which PTEN expression was reduced by siRNA. These results suggest that Pten deficiency leads directly to an altered VGF profile that may be responsible for the cardiovascular defects of *Tie2CrePten*$^{flox/flox}$ mice.

In *Tie2CrePten*$^{+/+}$ MLECs, expression levels of VEGF-A and its receptors VEGFR1 and VEGFR2 were significantly increased after stimulation with VEGF-A, as expected. However, this expression was further increased in *Tie2CrePten*$^{flox/+}$ MLECs (Fig. 4F). This enhanced expression of VEGF-A and its receptors may thus partly contribute to the enhanced angiogenesis observed in *Tie2CrePten*$^{flox/+}$ mice.

Partial rescue of Tie2CrePten$^{flox/+}$ *and* Tie2CrePten$^{flox/flox}$ *mice by null mutation of* p110γ *or* p85α

*p85*α is the most abundant and widely expressed regulatory subunit of the class IA PI3Ks. These kinases are

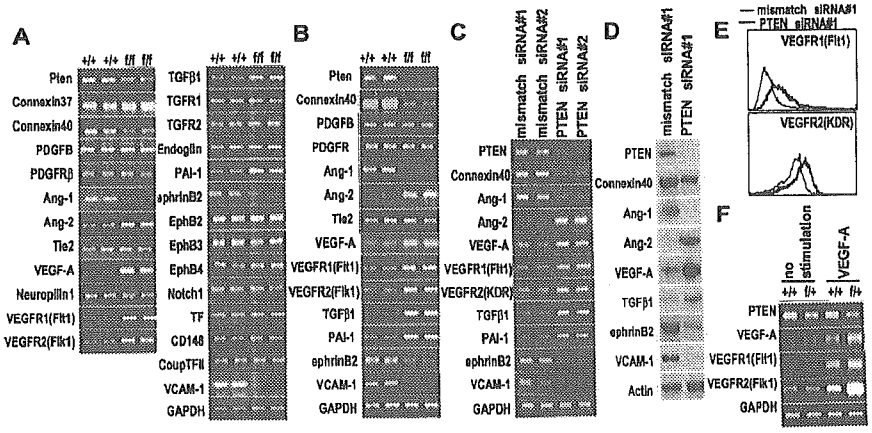

Figure 4. Expression of VGFs, VGF receptors, and their downstream molecules. RT–PCR and protein analyses of expression of the indicated molecules important for cardiovascular development are shown. (*A*) RT–PCR of whole wild type (+/+) or *Tie2CrePten*$^{flox/flox}$ (f/f) yolk sacs at E8.5. (*B*) RT–PCR of VEGFR2$^+$ cells from E9.5 +/+ or f/f embryos. (*C–E*) RT–PCR (*C*), Western blotting (*D*), and flow cytometry (*E*) of HUVECs transfected with PTEN siRNA or mismatched control siRNA. Pten deficiency resulted in significantly reduced expression of connexin 40, Ang-1, ephrinB2, and VCAM-1 but significantly increased expression of Ang-2, VEGF-A, VEGFR1, VEGFR2, TGF-β1, and PAI-1. (*F*) RT–PCR of VEGFR2$^+$ cells from E9.5 *Tie2CrePten*$^{+/+}$ (+/+) or *Tie2CrePten*$^{flox/+}$ (f/+) embryos that had been left untreated or stimulated with VEGF-A for 24 h. Pten heterozygosity in endothelial cells resulted in significantly increased expression of VEGF-A, VEGFR1, and VEGFR2. For *A–F*, data are representative of five independent experiments. GAPDH and actin served as loading controls.

activated following RTK engagement by VGFs. *p110*γ is the sole catalytic subunit of the class IB PI3K that is activated by the βγ subunit of G proteins. *p110*γ thus acts downstream of activated GPCRs (Stoyanov et al. 1995; Dimmeler et al. 1998; Morales-Ruiz et al. 2001). We generated *p85*α$^{-/-}$Tie2CrePten$^{flox/+}$, p85α$^{-/-}$Tie2CrePten$^{flox/flox}$, *p110*γ$^{-/-}$Tie2CrePten$^{flox/+}$, and *p110*γ$^{-/-}$Tie2CrePten$^{flox/flox}$ double mutant mice to clarify the contribution of class IA and class IB PI3Ks to the phenotypes observed in *Tie2CrePten*$^{flox/+}$ and *Tie2CrePten*$^{flox/flox}$ mice. Unexpectedly, homozygous mutation of *p110*γ partially restored control of angiogenic responses to *b*FGF, *b*FGF + Ang-1, and *b*FGF + VEGF in *Tie2CrePten*$^{flox/+}$ mice (Fig. 5A,B). Moreover, decreased tumor angiogenesis and tumor growth were observed in *p110*γ$^{-/-}$Tie2CrePten$^{flox/+}$ double mutants after inoculation of either LLC cells (Fig. 5C,D) or B16BL6 cells (data not shown). We then analyzed whether the failure of cardiovascular development observed in *Tie2CrePten*$^{flox/flox}$ mice was also *p110*γ-dependent. Homozygous loss of *p110*γ led to a dramatic rescue of all *Tie2CrePten*$^{flox/flox}$ phenotypes (Fig. 5E,F) such that the double mutant mice survived until E18.5–E19.5.

Homozygous mutation of *p85*α restored control of angiogenic responses in *Tie2CrePten*$^{flox/+}$ mice to the same degree as mutation of *p110*γ (Fig. 6A–D). However, the defect in cardiovascular morphogenesis seen in *Tie2CrePten*$^{flox/flox}$ mice was only partially rescued by *p85*α deficiency (Fig. 6E) such that these animals survived only until E14.5–E15.5.

Our data show that the enhanced angiogenesis exhibited by *Tie2CrePten*$^{flox/+}$ mice involves both *p85*α and *p110*γ, while the defect in cardiovascular morphogenesis in *Tie2CrePten*$^{flox/flox}$ mice depends more strongly on *p110*γ than on *p85*α. We conclude that the interaction of PI3Ks and Pten is essential for the regulation of cardiovascular morphogenesis and post-natal neovascularization, including tumor angiogenesis.

Discussion

Heterozygous Pten deficiency in endothelial cells accelerates tumor growth by enhancing tumor angiogenesis

Angiogenesis is a tightly regulated event critical for tumor growth. Tumor angiogenesis requires the activation, proliferation, and migration of endothelial cells, tube formation, and tissue infiltration by preexisting blood vessels. All these processes are controlled by angiogenic growth factors secreted either by the tumor or the surrounding stroma (Folkman and Shing 1992; Plate et al. 1994). Overexpression of VEGF, Ang-1, bFGF, and their receptors is strongly associated with invasion and metastasis in human cancers, and VGF inhibition blocks angiogenesis and tumor growth (Kim et al. 1993).

Our study is the first to demonstrate that the loss of Pten specifically in mouse endothelial cells makes them hypersensitive to VGFs and thus is responsible for enhanced angiogenesis leading accelerated tumor growth. An identical mechanism may be operating in humans with Cowden disease, a hereditary syndrome of cancer susceptibility caused by heterozygous mutations of *PTEN*. Our results have provided fresh insight into this syndrome and suggest that an individual who inherits a mutated *PTEN* allele is not only at risk for additional tumorigenic mutations due to the LOH of PTEN function but may also experience accelerated growth of any incipient tumors due to enhanced angiogenesis. Our findings thus further justify efforts to target PTEN and the PI3K–PKB/Akt pathway as a cancer therapy.

Homozygous Pten deficiency in endothelial cells causes a fatal vascular remodeling defect

The major downstream target of Pten is the survival kinase PKB/Akt, and PKB/Akt overexpression supports endothelial cell survival in vitro (Gerber et al. 1998). Transient activation of PI3K–PKB/Akt and subsequent acti-

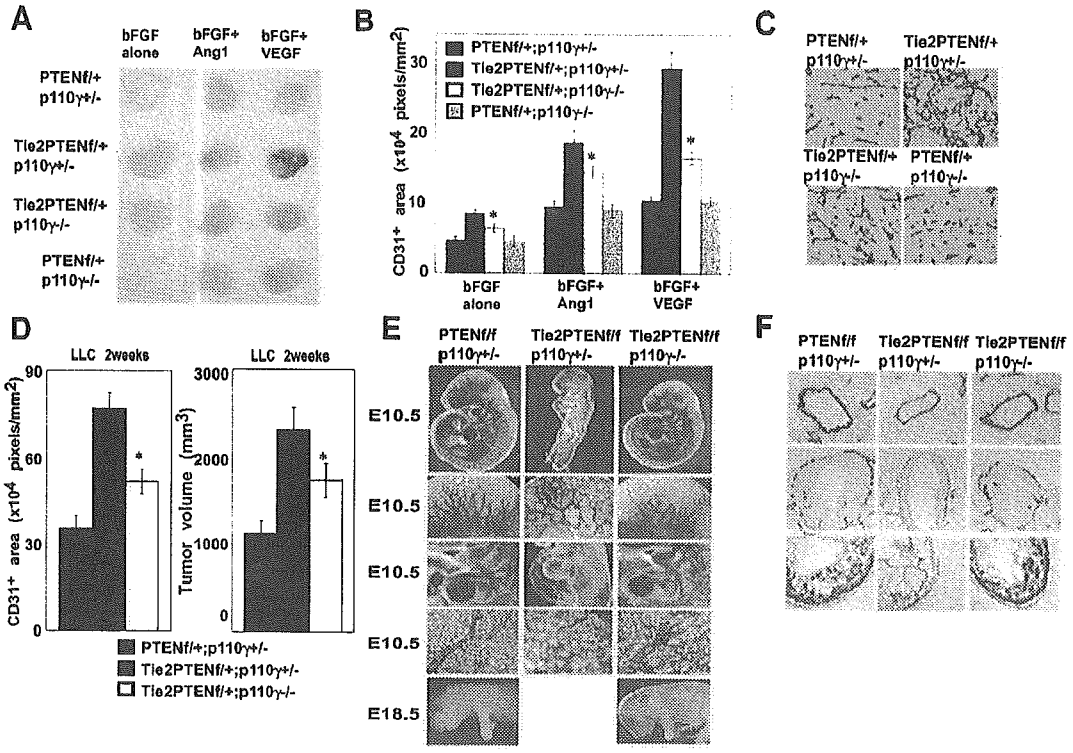

Figure 5. Partial rescue of Pten deficiency by *p110γ* deficiency. (*A,B*) Mitigation of increased angiogenesis driven by VGFs in *p110γ*$^{-/-}$*Tie2CrePten*$^{flox/+}$ mice. (*A*) Representative photos of Matrigel plugs containing *b*FGF, bFGF + Ang-1, or *b*FGF + VEGF-A. Plugs were removed from mice of the indicated genotypes at 14 d post-injection. (*B*) Quantitated vascularization of the Matrigel plugs in *A*. *p110γ* deficiency significantly decreases the plug vascularization response (n = 6/genotype). (*C,D*) Mitigation of increased tumor growth. Shown are the results of anti-CD31 staining of sections of LLC tumors (*C*), quantitated tumor vascularization (*D*, *left* panel), and tumor growth (*D*, *right* panel) at 2 wk post-LLC inoculation (n = 4/genotype). Loss of *p110γ* decreased the tumor vascularization and tumor volume observed in *Tie2CrePten*$^{flox/+}$ mice. (*E,F*). Partial restoration of cardiovascular development in *p110γ*$^{-/-}$*Tie2CrePten*$^{flox/flox}$ mice. Whole mounts stained with anti-CD31 antibody (*E*), and histological sections stained with α-SMA antibody (*F*) show that loss of *p110γ* dramatically rescues the growth retardation, vascular remodeling defect, reduction in vascular sprouting, enlarged pericardial cavity, and reduced thickness of the cardiac walls observed in *Tie2CrePten*$^{flox/flox}$ mice. For *B* and *D*, quantitative results are expressed as the mean ± SEM and are representative of three trials. Statistical differences were determined using the Student's t-test; (*) $p < 0.05$.

vation of eNOS by growth factors such as VEGF enhance endothelial cell migration, angiogenesis, tube formation, and vasorelaxation (Shiojima and Walsh 2002). Constitutively active PKB/Akt (myrAkt) expression in vivo causes fatal vascular malformations and bleeding due to a failure in vascular remodeling (Sun et al. 2005). Mice deficient for Foxo1, a transcription factor negatively regulated by PKB/Akt, also show fatal vascular remodeling and cardiac defects (Furuyama et al. 2004). These findings are strikingly similar to those obtained for our endothelial cell-specific Pten-deficient mice. The phenotypes observed in Foxo1-deficient mice were attributed to reductions in connexin 37, connexin 40, and ephrinB2 expression (Furuyama et al. 2004). Indeed, we also found decreased connexin 40 and ephrinB2 expression in our mutants. Mice deficient for ephrinB2 die at E10.5 due to defects in vascular remodeling and sprouting that lead to pericardial effusion or bleeding (Wang et al. 1998). Taken together, these data suggest that dysregulation of downstream targets of PKB/Akt and Foxo1 due to loss of Pten function may be responsible for the lethal phenotype of *Tie2CrePten*$^{flox/flox}$ mice.

The recruitment of PCs/vSMCs may determine the transition from an immature to a mature capillary network (Jain 2003) via a process regulated by factors such as PDGF (Lindahl et al. 1997), Ang-1 (Suri et al. 1996), and TGF-β1 (Dickson et al. 1995). If the gene dosage of PDGF-B is reduced by half, a modest increase in acellular capillary formation occurs (Lindblom et al. 2003). However, both PDGF-B and its receptor PDGFRβ were normal in *Tie2CrePten*$^{flox/flox}$ mice. Disruption of Ang-1 or its receptor Tie2 in knockout mice causes vascular defects due to impaired recruitment of PCs/vSMCs (Dumont et al. 1994; Suri et al. 1996). The effects of Ang-1 are antagonized by Ang-2 since Ang-2 inhibits the autophosphorylation of Tie2 induced by Ang-1 (Maisonpierre et al. 1997). Indeed, administration of Ang-2 causes a dose-dependent PC "dropout" in the normal retina (Hammes et al. 2004). In our mutant mice, Ang-2 expression was markedly increased while that of Ang-1 was reduced, perhaps explaining the impaired recruitment of PCs/vSMCs. Normally, the interaction of endothelial cells and PCs/vSMCs drives expression of TGF-β1 (Antonelli-Orlidge et al. 1989). Mice lacking either TGF-